UNIVERSITY OF MINES AND TECHNOLOGY

TARKWA

FACULTY OF MINERAL RESOURCES TECHNOLOGY

DEPARTMENT OF GEOLOGICAL ENGINEERING

A THESIS REPORT ENTITLED

DELINEATING A MULTI-ELEMENT MINERAL DEPOSIT AT BALATINDI, GUINEA, USING GEOPHYSICS

BY

SULEMANA AMADU

Submitted in partial fulfilment of the requirement for the award of the degree of Master of Science in Geological Engineering

THESIS SUPERVISOR

……

ASSOC PROF ANTHONY EWUSI

TARKWA, GHANA

MAY 2019

DECLARATION

I, Amadu Sulemana, declare that this thesis is my own work. It is being submitted for the Degree, Master of Science in Geological Engineering in the University of Mines and Technology (UMaT), Tarkwa. It has never been submitted by any other person for any degree or examination in any other university.

…… (Signature of Candidate)

……. day of…… (Year)……...

ABSTRACT

Balatindi Mineral Prospect, Guinea, is a multi-element mineral prospect that hosts Gold, Uranium and Copper with a potential for commercial production. It is located in eastern Guinea within the Bale` mylonitic zone, a zone of transition between the Archean Kenema-Man domain and Paleoproterozoic Birimian domain. A major challenge for exploration activities in the Balatindi area is the turnaround time for assay results due to the unavailability of a nearby assay laboratory. This coupled with the increasing cost of laboratory sample analysis calls for the need to find a faster and cheaper way of delineating mineral anomalies within the Balatindi area. Magnetic susceptibility and radiometric surveys are the two geophysical techniques applied to delineate gold and uranium anomalies respectively, because of the rapid and cost-effective ways in which data is acquired. Additionally, these methods yield substantial quantity of accurate data, thus enhancing interpretation and deduction. Downhole drill data for 37 HQ size diamond drilled holes of about 9200 m were used for the analysis. Magnetic susceptibility data were taken for 13 diamond drilled holes from the Central Polymetallic Prospect (CPP) area, whiles radiometric data were taken for the 24 drill holes in anomaly A to E areas. The data were correlated with the laboratory assay results for gold and uranium respectively. Strip logs comprising trace shades, histograms and line graphs, and statistics were used to interpret magnetic susceptibility readings against gold assay values, and radiometric readings against uranium assay values. Maximum and minimum values of -2.46 X 10^{-3} and 546.5 X 10^{-3} magnetic susceptibility were respectively recorded whiles 45 and 7250 cps were the maximum and minimum radiometric readings recorded. There was an inverse correlation between negative magnetic susceptibility values and gold assay values, however, there were few of such values to draw a definite conclusion. Positive magnetic susceptibility values did not show any preferential correlation with gold mineralisation. Radiometric count per second showed a very strong direct correlation with uranium mineralisation because it is a function of radiometric mineral present and therefore, radiometric survey can be used as a faster and cost-effective way of delineating uranium anomaly within the Balatindi prospect.

DEDICATION

I dedicate this thesis to my late father Alhaji Amadu Mumuni Kurubari.

ACKNOWLEDGEMENTS

My profound gratitude to Assoc. Prof. Anthony Ewusi, my Supervisor of the Geological Engineering Department of UMaT, for his patience, guidance and effective supervision.

I am also grateful to Mr Jamel Seidu and Mr Derrick Aikins also of the Geological Engineering Department and Mr Richard Amoako of the Mining Engineering Department for their tutelage and guidance in producing this thesis.

My gratitude also goes to all the staff of the Geological Engineering Department of UMaT.

Much appreciation to the management and staff of Burey Gold Guinea, especially Mr Famoussa Kaba, Mr Kwaku Agyei Henaku and Mr Bernard Asare.

To my wife Christiana Gaanye and my children Abdul Samed, Mariam, Hadia and Amadu Junior, I love you.

Alhamdulilah

TABLE OF CONTENT

LIST OF FIGURES

LIST OF TABLES

CHAPTER 1

INTRODUCTION

1.1 Problem Definition

Burey Gold's Balatindi property is a highly prospective multi-element mineral deposit of the Iron Oxide, Copper, Gold and Uranium (IOCGU) type. Situated in the eastern part of the Republic of Guinea, it potentially hosts commercial quantities of Gold, Uranium and Copper. Two mineralised domains are observed at Balatindi. Gold-dominated mineralisation in the Central Polymetallic Prospect (CPP) is hosted within a granodiorite sheet sandwiched between two layers of Archaean quartz-amphibole gneiss, immediately north of an interpreted east-west trending thrust (Egal *et al.*, 2002). Uranium dominated mineralisation is developed south of the thrust.

The location of the Balatindi project presents a practical problem in terms of turnaround time for assay results. The closest analytical laboratory is located in Bamako, Mali, where it takes a minimum of three months to receive assay results. This in addition to the high cost of assay analysis presents a huge challenge in program planning and implementation, and therefore, a quicker and cheaper way of delineating anomalous zones is required for quick decision making in the field for a wide area exploration without having to wait for laboratory assay results. Geophysical methods; magnetic susceptibility and radiometric surveys, are the techniques considered in this regard.

Geophysics was considered because of the rapid and cost-effective ways in which geophysical data is acquired. Additionally, geophysical methods yield a substantial quantity of accurate data, thus enhancing interpretation and deduction.

Magnetic susceptibility detects subtle changes in composition that can be linked to paleoclimate-controlled depositional processes and mineralisation. The high precision with which these measurements are taken makes it extremely useful for core-to-core and core-downhole log correlation (Tarling and Hrouda, 1993). Similarly, radiometric survey is a very useful tool in delineating radiometric anomalies, particularly uranium, and lithological contacts (Gabor and Peter, 2011). The gamma count is a function of the concentration of radioactive elements in the rock.

The use of magnetic susceptibility in mineral exploration is an age-old practice that has proven successful in the delineation of mineralised zones. Tsiboah and Arko (1999) carried out magnetic susceptibility measurements on fresh rocks of the Birimian volcanic greenstones of the Ashanti Belt and observed a genetic relationship between magnetic susceptibility and gold mineralisation within the Birimian rocks of Ghana. Also, Wemegah *et al.* (2009b) carried out magnetic susceptibility characterisation on mineralised and non-mineralised rocks from the Subensu Concession of Newmont Ghana Gold Limited and detected a general decrease in the magnitude of magnetic susceptibility of rocks with increase in rock alteration and corresponding increase in gold assay values.

For many years, radiometric survey has been and is still the main tool for uranium exploration. Generally, ground radiometric surveys is used to isolate the sources of anomalies defined by airborne radiometric surveys.

In the North Shore Property Turgeon, Weegee Highway, Pontbriand and Ne Costebelle Claim Blocks Province of Quebec, Canada, Lafleur (2006) successfully delineated drill targets for uranium using data from radiometric survey that was carried out. Also, in the exploration for uranium at Wadi Um Laseifa area, Egypt, Ramadan *et al.* (2002) used the SPP 2 NF scintillometer to select high anomalous areas for rock sampling. This approach was successful in delineating the uranium anomaly.

Airborne gamma ray spectrometry and magnetic techniques were successfully used for mapping alteration and mineralisation zones in the granitic rocks of Gabal Dara area, Egypt (Gemail *et al.*, 2016). In addition, the natural dose rate was calculated and compared with stream networks and structural lineaments to define the potential hazards caused by anomalous distribution of natural radioelements.

From the forgoing, the use of magnetic susceptibility and radiometric survey techniques to delineate anomalies in mineral exploration have proven successful.

This research seeks to establish a relationship between magnetic susceptibility and radiometric survey with gold and uranium mineralisation in the Balatindi project and to use that relationship to delineate anomalous zones in a faster and cheaper way.

1.2 Objectives

The objectives of this project are to:

i. Establish a correlation between magnetic susceptibility and radiometric counts and, gold and uranium mineralisation respectively in the Balatindi prospect, and
ii. Establish a faster and cheaper way of delineating anomalous zones.

1.3 Methods Used

The methods used include:

i. Measurement of magnetic susceptibility and radiometric counts on the diamond drilled core from the Balatindi prospect;
ii. Acquisition of multi-element assay results for the diamond drilled core;
iii. Analysis of magnetic susceptibility and radiometric survey data;
iv. Plotting of down hole assay results, magnetic susceptibility and radiometric survey results using MapInfo Discover software;

1.4 Facilities Used

The facilities used for this project include:

i. SM30 susceptibility meter and S.P.P.2 NF Scintillometer from Burey Gold Ltd; and
ii. Internet and Library facilities of the University of Mines and Technology (UMaT), Tarkwa.

1.5 Report Organisation

This report is structured into six (6) chapters, Chapter 1 is the introductory chapter giving background information on the project, the statement of problem, objectives and methods used. Chapter 2 describes the project area and geological setting. Chapter 3 is a review of relevant literature on the methods used. Chapter 4 discusses the methods used for data collection. Data analysis is carried out in Chapter 5. Finally, the conclusions and recommendations are included in Chapter 6.

CHAPTER 2

THE STUDY AREA

2.1 Location and Accessibility

The Balatindi permit covers an E-W elongated rectangular area of some 249 km², which traverses a portion of the common boundary between Kerouane and Damaro-Odienne, and lies partly in each of the two administrative prefectures, Kankan and Kerouane.

The property is located 80 km south of Kankan, Guinea's second largest city and second capital, after Conakry. Kankan is the base for Burey Gold's regional office. Figure 2.1 shows the map of Guinea showing the Balatindi project location.

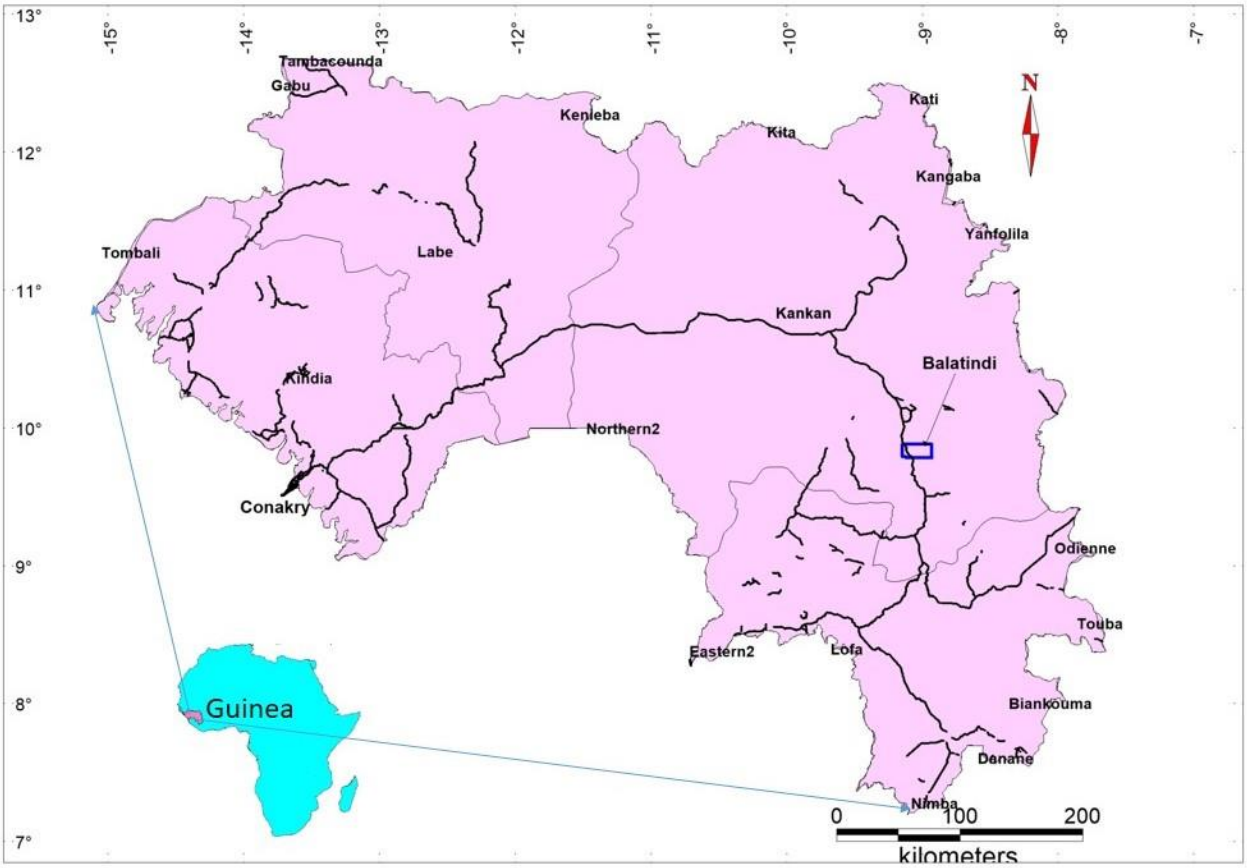

Figure 2.1 Map of Guinea Showing the Balatindi Project Location

2.2 Physiography, Climate and Economy

The Balatindi area falls within the Guinea interior highlands. The topography is undulating with elevations ranging between 300 and 700 m above sea level. It is drained by several easterly trending streams that are tributaries of the Dion River. The highest peak, the Balatindi Hill, dominates the middle part of the property.

The climate within the area is tropical with relatively high humidity throughout the year. Precipitation is generally high, about 1,200 mm annually.

Agriculture is the main occupation of the people, with more than 70% of the population engaged in subsistence farming.

The main export commodity is bauxite. Additional mineral exports are diamond and gold, much of which are extracted by the approximately 40,000 artisanal miners (Anon., 1999).

2.3 Regional Geology

The southern part of the West African Craton, where Guinea is located, comprises two distinct entities, namely the Archean Kenema–Man domain making up the south-western part of the craton, and the Paleoproterozoic Birimian domain forming the central and eastern parts (Kesse, 1985).

The Archean domain shows the superposition of at least two major tectono-magmatic cycles; these are the Leonian (~2900–3000 Ma) and Liberian (~2700–2800 Ma) cycles (Kouamelan *et al.*, 1997). The Paleoproterozoic Birimian domain, however, was established and structured during a single cycle, the Eburnean (~2200–2000 Ma) (Egal *et al*., 2002). According to Bohomme (1962), the term 'Eburnean' refers to all tectonic, metamorphic and plutonic events affecting the Birimian rocks during the Paleoproterozoic at about 2200– 2000 Ma. Figure 2.2 shows the geological map of the West African Craton showing the location of the Balatindi project area.

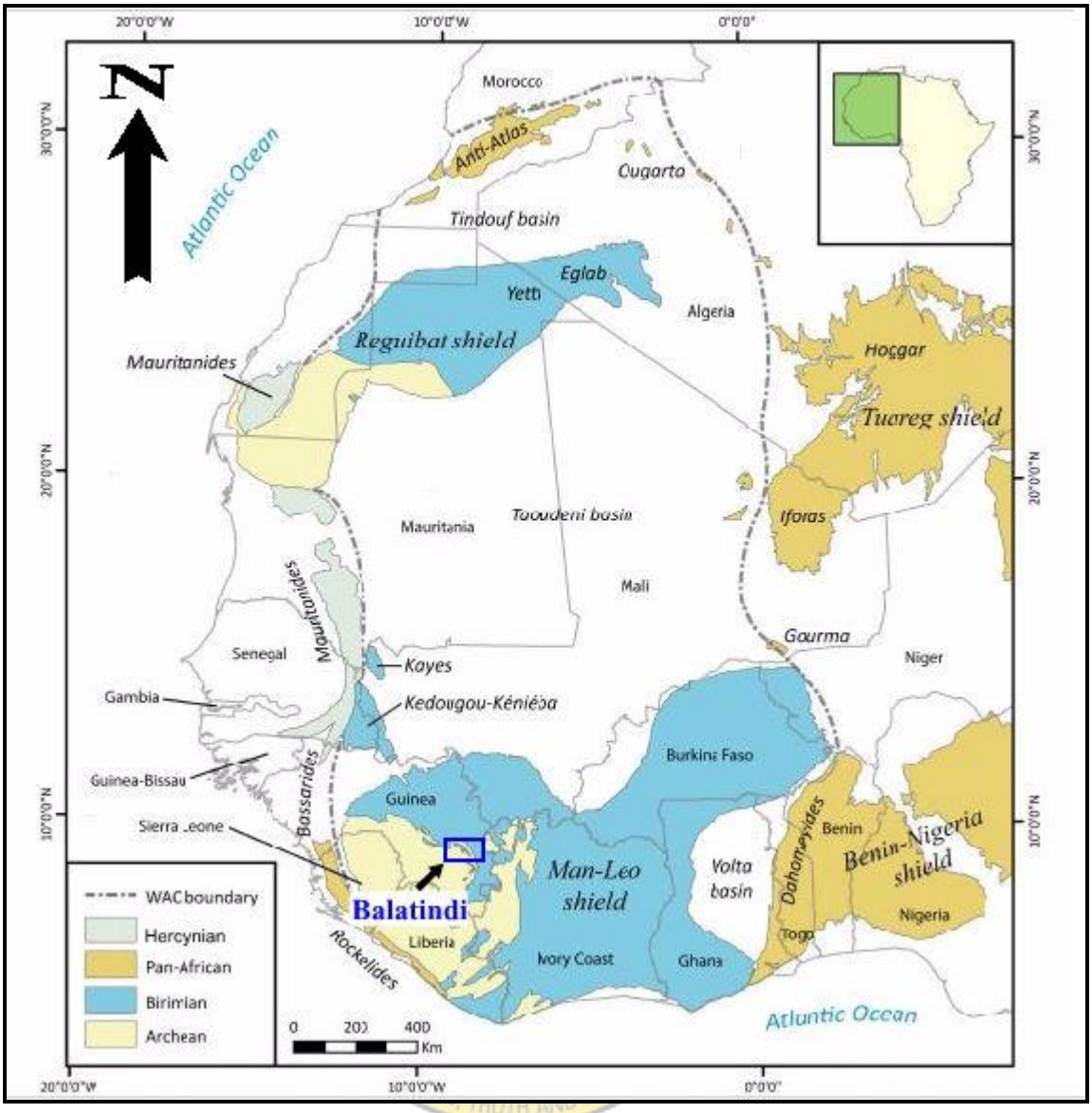

Figure 2.2 Geological Map of the West African Craton Showing the Location of the Balatindi Project Area (Grenholm, 2014)

Three units identified within the Archean, are;

1. A pre-Liberian (i.e. older than 2.8–2.9 Ga), high grade metamorphic succession (amphibolite to granulite facies), partially affected by retrograde metamorphism. An age of 3050±16 Ma has been obtained on zircons SHRIMP (Sensitive High Resolution Ion Probe) from an orthogneiss (Goujou *et al.*, 1999).
2. Two batholiths of Liberian age (2800–2900 Ma) (Thie´blemont *et al.*, 2001) occupy the western and south-eastern parts of the Guinean forest region. Towards the southwest in Liberia, the western batholith gives way to a batholith imprecisely dated at some 2650 Ma (Hurley *et al.*, 1971), whereas towards the east, the south-eastern

batholith gives way to granitic rocks of the Man domain (Ivory Coast) dated at about 2800 Ma (Camil *et al.,* 1983; Kouamelan *et al.,* 1997; Cocherie *et al.,* 1998) and,

3. Two Banded Iron Formation (BIF) units, the Nimba and Simandou successions, whose unconformable relationship over the Archean gneiss and granitic rocks has been confirmed (Lahonde`re *et al.,* 1999). These two ranges, made up essentially of metavolcanic and metasedimentary (mainly banded ferriferous quartzite) rocks, are now attributed to the late Archean/Early Proterozoic on the basis of maximum ages obtained on detrital zircons extracted from quartzite, i.e. 2615 Ma for the Nimba succession (Billa *et al.,* 1999) and 2711–2871 Ma for the Simandou succession (Thie´blemont *et al.,* 2001).

The early Proterozoic Siguiri Basin occupies a vast area in the northern part of eastern Guinea (Figure. 2.2 and Figure 2.3). It disappears to the north beneath Neoproterozoic sediments of the Taoude´ni Basin. Along the southern edge of the basin, granitic–gneissic rocks assigned to the Archean are exposed in local tectonic thrust slices. The Siguiri Basin is essentially composed of marine detrital sedimentary rocks (argillite to fine-grained sandstones) and, to a lesser degree, volcanic rocks (lava and pyroclastics) intercalated within these sediments, and subvolcanic dykes (Egal *et al.,* 2002).

According to Hirdes *et al.* (1992), no evidence exists to suggest the presence of an Archean basement under the Paleoproterozoic domain. The boundary between the Archean and Paleoproterozoic domains (Figure. 2.3) is traditionally identified as the Sassandra Fault in the southern part of the craton and less precisely, as the southern boundary of the Birimian Basin of Upper Guinea (Siguiri Basin) in the northern part. Nonetheless, recent work undertaken in the Ivory Coast (Kouamelan *et al.,* 1997) and south-eastern Guinea (Billa *et al.,* 1999) has revealed an extension of Paleoproterozoic (Eburnean) tectonism and granitisation into the actual Archean domain. This Archean/Proterozoic transition zone is often referred to as the Balé Mylonitic Zone. The Balatindi Project is located within the Balé Mylonitic Zone.

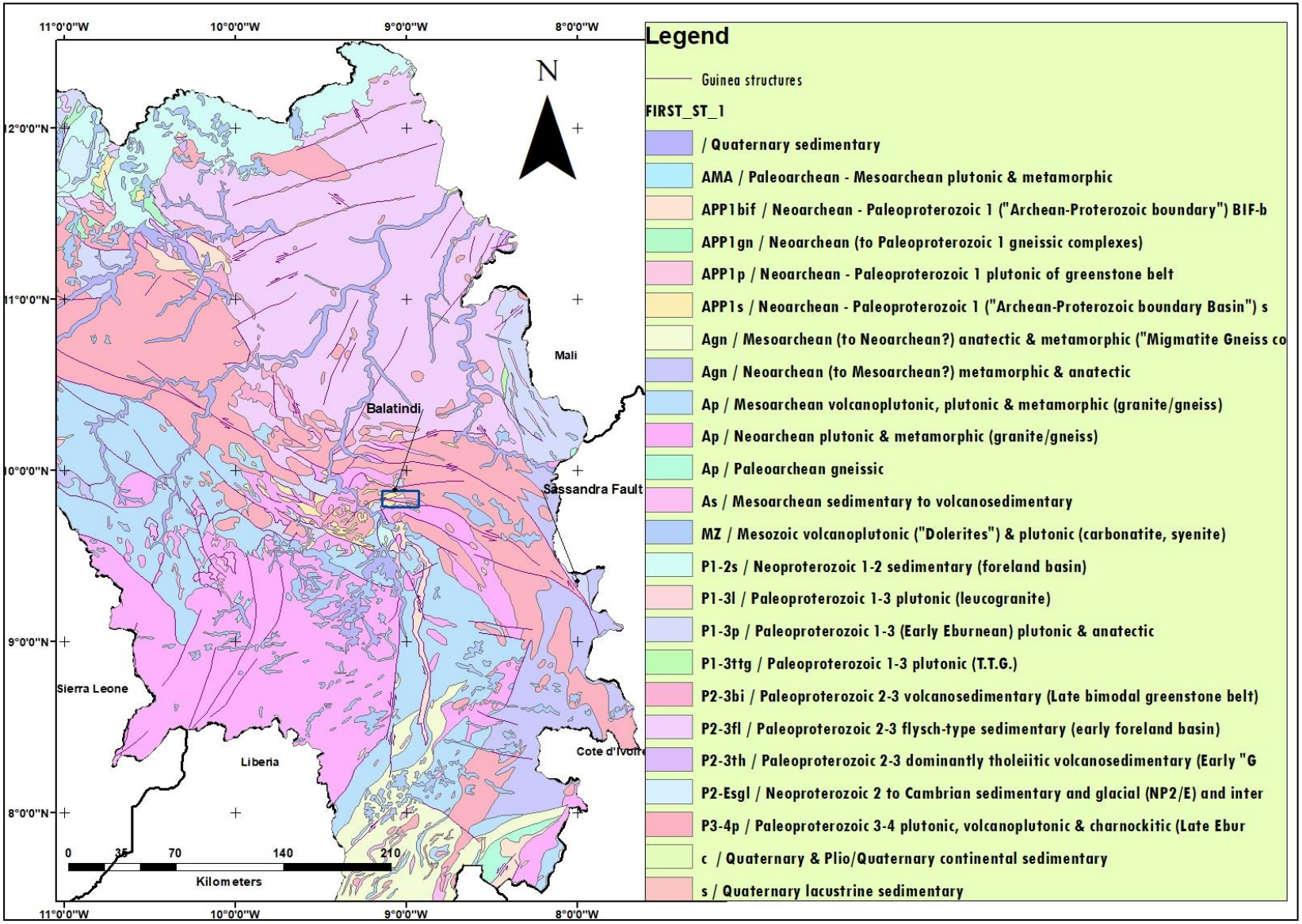

Figure 2.3 Simplified Geological and Structural Map of Eastern Guinea.

2.4 Local Geology

The Balatindi Project is located in eastern Guinea within the Balé Mylonitic Zone. This zone forms part of a broad tectono-magmatic belt developed between the Archaean Kénéma-Man Craton to the south and the Paleoproterozoic Birimian Siguiri Basin to the north. The belt rims the margin of the Craton in eastern Guinea. In the region around Balatindi, the belt is 50km to 100km wide and trends east-west to northwest-southeast for approximately 150km. It is late Eburnean in age and comprises a variety of pre-tectonic to syn-tectonic granitic rocks (granodiorite, biotite granite, monzogranite and two-mica granite) with an anastomosing network of major northwest-southeast trending ductile sinistral strike-slip fault zones characterised by intense mylonitic to ultramylonitic deformation. This tectono-magmatic belt is considered to have undergone deformation during regional shortening towards the west southwest, which was mainly accommodated by sinistral strike-slip movement (Robertson and Witley, 2013).

Based on the chemistry of the granitic rocks within this belt, Egal, *et al.* (2002) consider it similar to magmatic suites developed on active margins above subduction zones. Evidence of strong contamination from the Archaean Kénéma-Man Craton supports emplacement of the plutonic belt directly above a subduction zone. This is the classic setting for the generation of porphyry type mineral deposits (Robertson and Witley, 2013).

Local mapping within Balatindi found gneiss, granodiorite, monzonite, basalt and andesite as the major rock types outcropping in the property. Diamond drilling however, reveal a wide variety of rock units that do not outcrop on surface such as volcaniclastic, dacite, greywacke and rhyolite.

In the Central Polymetallic Prospect (CPP), a granodiorite sheet is sandwiched between two layers of Archaean quartz-amphibole gneiss immediately north of an interpreted east west trending thrust. This area hosts the Gold mineralisation. Uranium-dominated mineralisation is developed south of the thrust at Anomalies A, B, C, D and E (Robertson and Witley, 2013). Figure 2.4 is the geological map of the area showing the Central Polymetallic Prospect (CPP) and anomalies A, B, C, D and E.

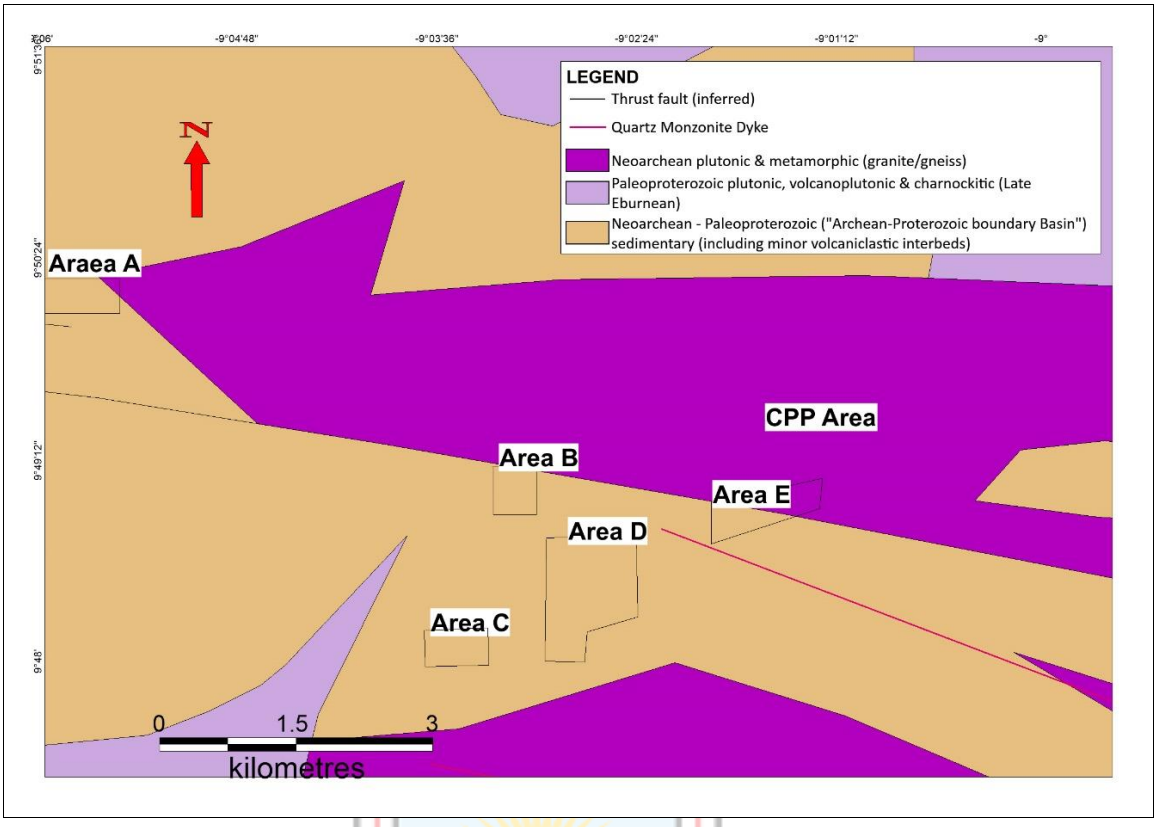

Figure 2.4 Geological Map of the Balatindi Project Area

2.5 Mineralisation Model

The setting of Balatindi within a tectono-magmatic belt adjacent to an interpreted active margin and overlying a subduction zone represents a classic setting for porphyry deposits, although porphyry deposits in Paleoproterozoic-age rocks are uncommon. However, Mesozoic Andean-type Iron Oxide, Copper and Gold (IOCG) deposits occur in a similar tectonic setting (Robertson and Witley, 2013).

Although the element association of the two mineral systems is similar to the typical geochemical association observed in IOCG deposits, iron contents are low, with a typical range (based on the Burey multi-element data) of 2-4% Fe, with an average of 2.85% Fe. Further, there appears to be little evidence for hydrothermal brecciation in the Balatindi system.

Mining Italiana viewed mineralisation in terms of a porphyry model, with a yet to be discovered porphyry body and mineralisation associated with hydrothermal fluids (Ransome, 2004). According to Robertson and Witley (2013), the Balatindi system

appears to be a hybrid between an IOCG and porphyry model; however essentially the same exploration approach would be required in terms of delineating these types of deposits.

At Anomaly E, uranium and copper show a close correlation, a function of mineralisation occurring as torbenite (a U-Cu phosphate). Uranium-copper mineralisation occurs in sub parallel zones which dip to the south at approximately 45°. The mineralisation follows an east-west trend aligned with the radiometric anomaly, with a sinistral displacement along a northeast trending fault (Anon., 2010). Mineralisation is developed over a combined strike length of approximately 400 m and appears to be open along the east-west trend; however, the radiometric anomaly suggests a limited strike extent.

CHAPTER 3

LITERATURE REVIEW

3.1 Magnetic Susceptibility

Understanding magnetisation is core in the study of magnetic susceptibility. Two types of magnetisation exist, viz: Remanent (permanent) magnetisation, which can have any direction, and Induced magnetisation, which is proportional to the susceptibility of the material being magnetised and which has the same direction as the Earth's field (Clark, 1997).

The Earth's magnetic field (Figure. 3.1), also known as the geomagnetic field is the magnetic field that extends from the earth's interior to where it meets a stream of charged particles emanating from the sun known as solar wind. The magnitude at the earth's surface range from 25 to 65 microteslas (0.25 to 0.65 gauss) (Palm, 2011).

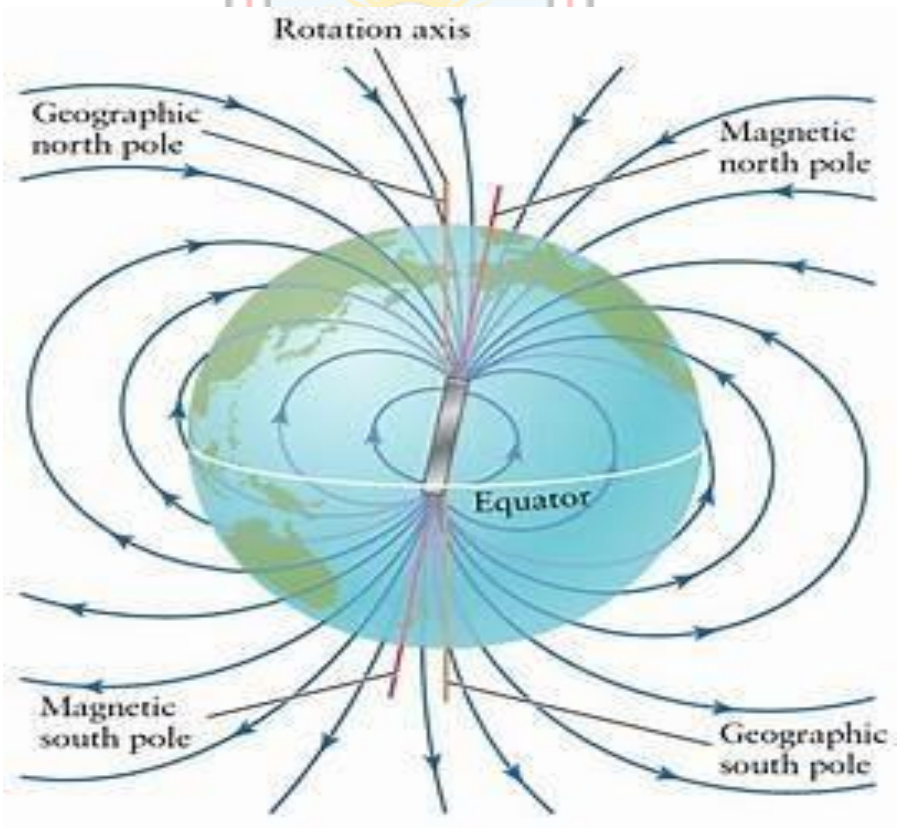

Figure 3.1 The Earth's Magnetic Field (Palm, 2011)

Magnetic susceptibility describes the ability of a substance to be magnetised when exposed to external magnetic field. In magnetically isotropic substances, it is defined as

$$M = k\,H \qquad (3.1)$$

Where M represents the vector of the induced magnetisation (in SI of units in A/m), H is the vector of the intensity of magnetic field (also in A/m) and k is the magnetic susceptibility (dimensionless scalar entity) (Hrouda *et al.*, 2009).

When a body is placed in a magnetic field it becomes a magnet as the atoms and molecules realign. Magnetic field induced in the body is called the induced or intensity of magnetisation. If the induced magnetisation has the same amplitude and direction throughout a body, the body is said to be uniformly magnetised. Positive values of magnetic susceptibility k imply that the induced magnetic field, M is in the same direction as the inducing field, H. Negative values of k imply that the induced magnetic field is in the opposite direction to the inducing field.

Materials can be classed into three groups according to their magnetic structure, these are; Diamagnetic materials whose magnetic susceptibility is negative, Paramagnetic materials have positive susceptibility, but generally low and Ferromagnetic materials which have high magnetic susceptibility (Tarling and Hrouda, 1993). Ferromagnetic materials are the most important in paleomagnetism in that they carry remenant magnetism. Figure 3.2 shows the relationship between the three types of magnetic materials.

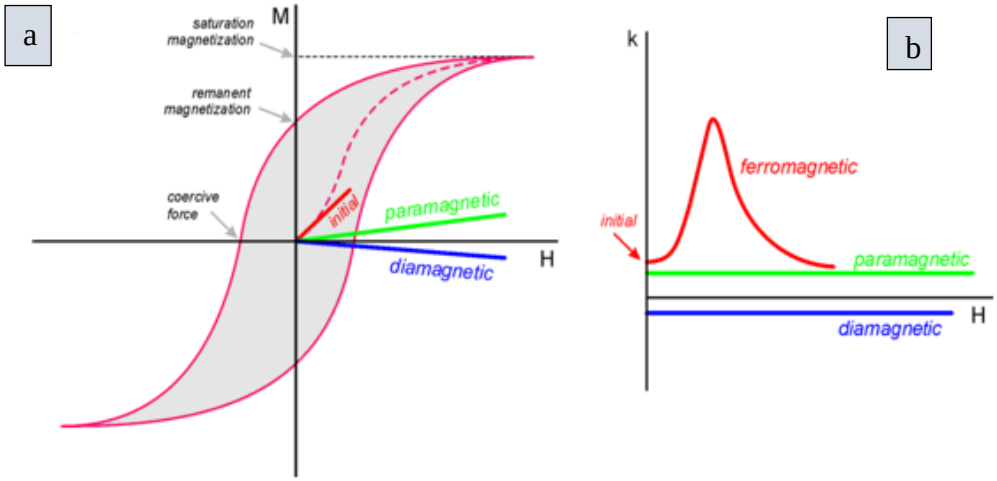

Figure 3.2 Relationship between Magnetisation and Intensity of Magnetising Field for a). Ferromagnetic, Paramagnetic and Diamagnetic substances and b). Field Variation of Susceptibility for the same Substances. (Hrouda, *et al.*, 2009)

Lindsley *et al.* (1966) assert that magnetic susceptibility is generally related to the magnetite content of rocks, but according to Hrouda *et al.* (2009), magnetic susceptibility of rocks is in principle controlled by the type and amount of magnetic minerals contained in a rock. Sometimes, it is dominantly controlled by paramagnetic minerals (mafic silicates such as olivine, pyroxenes, amphiboles, micas, tourmaline, garnets), often by ferromagnetic minerals (iron oxides or sulphides, represented for instance by magnetite and/or pyrhotite, respectively) and much less frequently by diamagnetic minerals (calcite, quartz). As the ferromagnetic minerals mostly belong to accessory minerals that are often sensitive indicators of geological processes, the magnetic susceptibility is a useful parameter in solving some petrologic problems (Hrouda *et al.,* 2009). Magnetic susceptibility has been applied in many fields of geoscience, from geological mapping to delineation of mineral anomalies.

3.1.1 Types of Magnetic Susceptibility

Volume susceptibility

The volume magnetic susceptibility, represented by the symbol $X_{v,}$ is defined by the relationship

$$M = X_v H \tag{3.2}$$

Where *M* is the magnetisation of the material (the magnetic dipole moment per unit volume), measured in amperes per meter, and *H* is the magnetic field strength, also measured in amperes per meter.

Measurement of susceptibility

There are two other measures of susceptibility, the mass magnetic susceptibility measured in $m^3 \cdot kg^{-1}$ in SI or in $cm^3 \cdot g^{-1}$ in CGS and the molar magnetic susceptibility Xmol measured in $m3 \cdot mol^{-1}$ (SI) or $cm^3 \cdot mol^{-1}$ (CGS) that are defined in equation (3.3) and equation (3.4), where ρ is the density in $kg \cdot m^{-3}$ (SI) or $g \cdot cm^{-3}$ (CGS) and M is molar mass in $kg \cdot mol^{-1}$ (SI) or $g \cdot mol^{-1}$ (CGS) (Heidelberg, 1986).

$$Xmass = Xv / \rho \tag{3.3}$$

$$Xmol = M\ Xmass = M\ Xv / \rho \tag{3.4}$$

Tensor susceptibility

The magnetic susceptibility of most crystals is not a scalar. Magnetic response M is dependent upon the orientation of the sample and can occur in directions other than that of the applied field H. In these cases, volume susceptibility is defined as a tensor susceptibility

$$Mi = XijHj \qquad (3.5)$$

Where *i* and *j* refer to the directions of the applied field and magnetisation, respectively.

3.1.2 Magnetic Susceptibility of Minerals

Except for rare monomineralic rocks, rocks consist in general of all three kinds - i.e. diamagnetic, paramagnetic and ferromagnetic minerals. Table 3.1 shows the susceptibility of the most frequent rock-forming and accessory minerals. It gives an idea of the contribution of individual minerals to the magnetic susceptibility of a rock. Figure 3.3 shows the contributions of individual minerals to the rock susceptibility as function of the content of the individual minerals in a rock. From Table 3.1 and Figure 3.3 it is clear that in strongly magnetic rocks, i.e. those with susceptibility higher than 5×10^{-3}, the rock susceptibility is controlled mostly by the presence of ferromagnetic minerals. In rocks with the lower susceptibility, the susceptibility may be controlled by both paramagnetic and ferromagnetic minerals, according to the rock mineral composition.

In some almost monomineralic rocks, such as limestone, marble, quartzite, if the content of ferromagnetic and paramagnetic minerals is very low or zero, the susceptibility can be negative, being controlled by the presence of diamagnetic calcite or quartz. In many minerals, the susceptibilities presented in Table 3.1 are not single values, but rather wide susceptibility intervals. This reflects variability of susceptibility with chemical composition of the minerals. For example, in orthopyroxene, the susceptibility is very low in the member free of iron, while in the member which contains no magnesium, it is relatively high. In general, the susceptibility depends on the ratio of Mg to Fe components as shown in Figure.3.3 (b). Similar situation exists in olivine, garnets and amphiboles. In titanomagnetites, the susceptibility depends on the amount of the titanium in the mineral (generally, it decreases with increasing Ti content, see Figure. 3.3).

Table 3.1 The Magnetic Susceptibility Variation of Individual Minerals (Bleil and Peterson, 1982)

Mineral	Susceptibility [10^{-6}] unit	Mineral	Susceptibility [10^{-6}] unit
Forsterite	-12.6	Sphene	264
Fayalite	4,976	Zircon	-15 to 386
Olivine	124 to 4,270	Quartz	-15.4
Enstatite	121	Opal	-12.9
Ferrosilite	3,670	Orthoclase	-13.7
Orthopyroxene	3,700	Halite	-10.3
Diopside	1,319	Apatite	-10.6
Hedenbergite	2,783	Graphite	-177
Augite	555 to 1,111	Aragonite	-15.0
Clinopyroxene	613 to 25	Calcite	-13.1
Actinolite	490	Dolomite	11.3
Arfvedsonite	3,468	Siderite	2,770 to 3,170
Riebeckite	3,016	Spinel	30
Hornblende	746 to 1,368	Chromite	2,827 to 7,069
Muscovite	36 to 711	Franklinite	5,750 - 3,000,000
Biotite	873 to 3,040	Jacobsite	50,000 to 3,000,000
Phlogopite	176 to 281	Magnetite	3,000,000
Lepidolite	136 to 1,560	Maghemite	up to 3,000,000
Pyrope	502	Rutile	107
Almandine	2,510 to 6,230	Ilmenite	8,042
Spessartite	6,780	Hematite	1,300 to 7,000
Andradite	2,280 to 4,320	Pyrite	-6.3 to 63
Garnet	553 to 6,230	Marcasite	61 to 245
Staurolite	790 to 1,590	Galena	-33 to 9.3
Cordierite	200 to 1,100	Sphalerit	-15 to 2,060
Tourmaline	39 to 1,520	Chalcopyrite	308 to 411
Beryl	23	Pentlandite-folgerite 1	00,057
Epidote	1,010	Gersdorffite	214 to 1,571
Orthite	970 to 3,960	Cobaltite	553 to 157,892

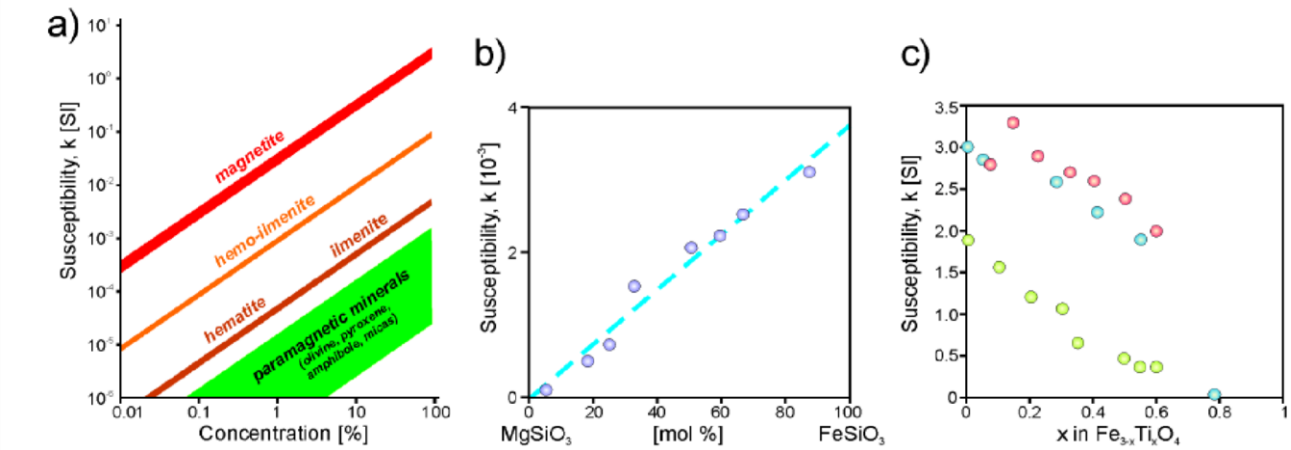

Figure 3.3 Contribution of Individual Rock Forming Minerals to Total Magnetic Susceptibility of the Rock in Terms of a). Mineral contribution, b). Chemical Composition in Orthopyroxene and c). Chemical Composition in Titanomagnetite

3.1.3 Reasons to Measure Magnetic Susceptibility

Magnetic susceptibility is easily and quickly measurable, and one can execute numerous detailed measurements in reasonable time. Furthermore, susceptibility measurement enables us to detect subtle changes in magnetic mineral content within the geological body or outcrop that are not macroscopically observable. In this way, cryptic magnetic and non-magnetic layers, lenses, enclaves and other bodies can be identified as well as gradual changes in the content of magnetic minerals (Hrouda *et al.*, 2009).

The appearance of a rock does not determine its magnetic susceptibility. Even though the mafic rocks show in general higher susceptibility than felsic rocks, there are many examples of light granites being both weakly and strongly magnetic. On the other hand, some dark rocks as gabbro and lamprophyres can be weakly magnetic. In addition, Fe ores with magnetite have high susceptibility, while the Fe ores with dominating hemoilmenite and having the same Fe content can show much lower susceptibility. Because of all these phenomena, it is recommended to measure the susceptibility in the field on rock outcrops (Hrouda *et al.*, 2009). Also, magnetic susceptibility depends on geochemical or mineralogical composition of the rocks and on later metamorphic processes and alterations. Very important controlling factors are also fugacities of O_2 and S. Magnetic susceptibility provides us with invaluable information in this respect (Evans and Heller, 2003).

3.1.4 Magnetic Susceptibility Meters

There are a number of magnetic-susceptibility meters available on the market. However, the instrument specifications defined by the respective manufacturers show there are significant differences between individual instruments, which may affect the reported magnetic-susceptibility value. Instrument-design variations include factors such as dimensions and position of the sensor coil and frequency of the current used to activate the coil. A few of them are discussed.

Bartington MS2E

The MS2E magnetic-susceptibility meter manufactured by Bartington Instruments Ltd. is a portable meter that may be used with rechargeable batteries or a main power supply. The Bartington tool comprises two elements: a) the MS2E meter and b) a sensor package that is linked by a cable to the meter. This design allows for a variety of sensor configurations. Variations in the geometry and dimensions of the sensor coil allow the user to tailor a measurement to a specific application. Specific sensor and coil geometries are offered for each of the following types of specimens: soil or rock samples, larger diameter drill cores, soil surfaces, and rock outcrops; the instrument can even be employed down auger holes. The sensor only weighs 0.22 kg, while the meter weighs 1.2 kg. The sensor element, which is located within a ceramic cylinder, is a rectangular coil (3.8 mm x 10.5 mm) that corresponds to a total sensing area of 39.9 mm^2. The small size of the sensor means that it is possible to precisely locate the coil over localized variations within an outcrop. The operating frequency for the coil is 2 kHz. The MS2E incorporates a standard correction for volume, giving it a sensitivity of 1 x 10^{-5} SI units (volume specific) or 1 x 10^{-8} SI units (mass specific). Instrument calibration is provided by reference to a 15 mm x 33 mm Fe_3O_4 disc in alumina and epoxy resin provided by the manufacturer. The measurement does not include corrections for the volume or mass of the sample. Shown in Figure 3.4 is a picture of the MS2E set up for the measurement of the magnetic susceptibility of a drill core.

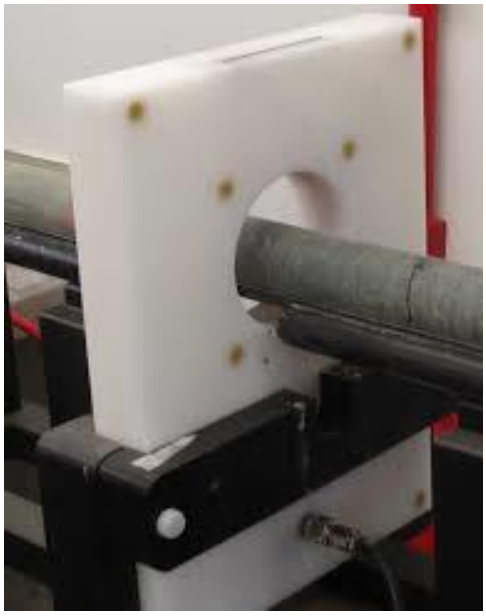

Figure 3.4 Picture of the MS2E Magnetic Susceptibility Meter

Heritage Geophysics SM-30

The SM-30 magnetic-susceptibility meter by Heritage Geophysics Inc is a small, compact hand-held field meter that weighs only 0.180 kg, ideal for outcrop measurements. This instrument has a 50 mm diameter detector coil, corresponding to a sensing area of 1964 mm^2, which is incorporated in the body of the meter. The exact location of the sensor coil in the body of the meter is not exactly known and there is no external measurement trigger (pin) as in the KT-10. The sensor coil has an operating frequency of 9 kHz and a sensitivity of 1 x 10^{-7} SI units. The instrument output does not include any correction for sample volume or mass. Figure 3.5 is a picture of the hand held SM 30

Figure 3.5 SM 30 Magnetic Susceptibility Meter

Terraplus KT-10

The KT-10 magnetic-susceptibility meter by Terraplus Inc. is a hand-held field meter designed for measurements on outcrops, drill cores, and rock samples. The KT10 is much bigger than the SM-30, and at 0.30 kg weighs almost twice as much. The inductive coil of the KT-10, which has a diameter of 65 mm corresponding to a total sensor area of 3318 mm^2, is located at the end of the instrument. The KT-10, shown in Figure 3.6, is designed to be used either with the standard pad that is equivalent in diameter to the inductor coil or with an attachable pin that holds the meter parallel to the rock surface to increase accuracy over uneven samples. This meter utilizes an operating frequency of 10 kHz with a sensitivity of 1 x 10^{-6} SI units. No volume or mass correction is performed by the operational software. Unlike other units, the KT-10 does include a GPS sensor that allows the user to tie a measurement to an observation location

Figure 3.6 KT-10 Magnetic Susceptibility Meter

3.1.5 Measuring Magnetic Susceptibility

Superficially, measurement of magnetic susceptibility might seem to be a simple procedure; that is, one holds the instrument in contact with a rock surface for a specific period of time while the instrument measures the change in frequency of the input signal caused by the presence of magnetic material. In practice, there are a number of operational complexities that need to be considered. These include;

1 When taking a measurement in the field, it is imperative to choose a flat surface in order to ensure optimum coupling between the inductive coil and the rock surface. The MS2E,

having a smaller coil, can acquire more accurate readings than the other two instruments on surfaces having greater curvature. Although the KT-10 has the largest coil diameter, it includes a ‘pin’ option that is intended to help guide the user in finding the best coupling between the rock surface and the coil.

2 In a natural setting, the mineralogy in the immediate near surface of a rock outcrop may have been modified by weathering. Often that weathering might include alteration of magnetite to less magnetic hematite, or more magnetic maghemite. The depth extent of the weathering rind is dependent on rock type and the location of the observation point. Therefore, measurement on a fresh surface (in the field or in the lab) is ideal if possible.

3 Each susceptibility observation is a summation of all magnetic-mineral contributions that are activated by the inducing coil. The number of magnetic grains examined in a measurement is controlled by various factors: with respect to the instrument, the frequency of the input signal, the number of turns of wire in the sensor coil, and the size of the coil; with respect to the sample, the size and concentration of magnetic grains. Bartington, for example, offers a coil (MS2B) designed for taking measurements on core samples that can operate at two frequencies: 0.465 kHz and 4.65 kHz. The ratio of these two readings, which is defined as ‘frequency-dependent’ susceptibility, is related to the grain-size distribution of magnetite in the rock sample. Varying the size of the inducing coil means that susceptibility is averaged over different volumes of material. Given multiple measurements of susceptibility on any given rock surface, the observed value will depend on the homogeneity of the rock with respect to the dimension of the sensor coil. That is, the smaller MS2E sensor should detect more detailed variation than the larger KT-10.

4 Measurements dependent on frequency changes in an inductive-coil circuit are known to drift. Obtaining reliable magnetic-susceptibility readings involves minimization of instrument drift and absolute calibration of the observed frequency change in terms of susceptibility. Each instrument permits different measurement methods, including interpolation and scan mode. An interpolation method is used for the KT-10 and SM-30 measurements, whereby a free-air measurement is taken, followed by a direct measurement on a rock sample or outcrop, and finally a second free-air measurement, where the first and third measurements are compensation steps The MS2E measurements were determined using a more extended interpolation mode where a preliminary free-air measurement was followed by up to three sample.

3.1.6 Application of Magnetic Susceptibility in Mineral Exploration

In the Hishikari epithermal gold deposit, Murakami (2007) successfully used magnetic susceptibility to identify hydrothermally altered zones, including alteration halos close to quartz veins. Magnetic susceptibility was used to detect magnetic changes in minerals, oxidation and phase transition (Plimer, 1985). Evans and Heller (2003), utilised magnetic susceptibility to detect loess lithological sequences caused by climate changes, and also to find and limit the effect of heavy metal pollution. Boroomand *et al.* (2015), accessed two methods of determining gradient tensor; different distance method and Fourier transform technique. From the investigation, the Fourier transform method was more consistent with the geological features which led to more reliable information required for mineral exploration.

Locally, mineralogical and statistical analysis was used by Kuma *et al*. (1999) to estimate the magnetic susceptibility of rocks in the concession of the Bogoso Gold Limited, and they concluded that metatuff had the lowest magnetic susceptibility whilst dolerite dyke recorded to highest susceptibility. Also, their work revealed that weathering had significantly reduced the susceptibility of the rocks and that the presence of graphite in the rocks had no effect on their overall susceptibility but pyrite had a small positive effect on them.

3.2 Radiometric Survey

Radiometric surveys and maps are applicable in several fields of geo science. They retain their geological and geophysical information for mineral prospecting, geochemical mapping and structural geology, and enable the comparison of geological features over large regions. Although the gamma ray method was originally developed for geoscience, it has also been successfully applied in emergency situations for mapping the contamination from nuclear fallout and for the location of lost radioactive sources (Anon., 2003).

Gamma ray spectrometry as a tool for mapping radioelement concentrations has found widespread acceptance in diverse fields. The method has evolved over several decades and continues to be developed. The method has benefited from continuing advances in instrumentation, field procedures, and calibration and data processing procedures. Gamma ray spectrometry is widely used for environmental mapping, geological mapping and

mineral exploration (Anon., 2003). The application of radioactivity in geoscience is based on knowledge of the physical properties of radiation sources, and our ability to detect these sources through the analysis of remotely sensed data.

3.2.1 Basic Radioactivity

Atoms are the smallest particles of mass with distinctive chemical properties. An atom consists of a nucleus surrounded by electrons. The nucleus is made up of positively charged protons, and uncharged neutrons. The diameter of an atom is of the order 10^{-10} m, and the diameter of a nucleus is of the order 10^{-15} m. Protons and neutrons have a mass of 1.67 X 10^{-27} kg. The mass of negatively charged electrons is 9.11 X10^{-31} kg. The elementary charge is 1.602 X 10^{-19} C. The number of protons in a nucleus of an element, X, is the proton number Z (also called the atomic number). The sum of the protons and neutrons (nucleons) is the mass number, A, of an atom. Atoms of an element having the same atomic number but different numbers of neutrons (i.e. different mass numbers) are called *isotopes*. Isotopes are denoted by their chemical symbol and their mass number as follows - ^{A}X. Isotopes have identical chemical properties, but different physical properties. Atoms having identical numbers of protons and neutrons are called nuclides. The atomic nuclei of some isotopes have a surplus of energy, are unstable, and disintegrate to form more stable nuclei of a different isotope. This process is accompanied by the emission of particles or energy, termed nuclear radiation. Nuclides with this feature are called radionuclides, and the process is called nuclear decay or disintegration. The radioactivity decay law expresses the decrease in the number of atoms of a radionuclide with time:

$$Nt = N_0\, e^{-\lambda} \qquad (3.6)$$

Where;

N_t = the number of atoms present after time t (s);

N_0 = the number of atoms present at time t = 0;

λ = the decay constant of a radionuclide (s_{-1}),

A related constant, the half-life $T_{1/2}$ (s), is the time taken for half the radionuclides initially present to decay: $T = 0.693/\lambda$

The product λN gives the activity (Bq) of the radionuclide. Radioactive decay is independent of other physical conditions.

3.2.2 Radioactive Decay

Several types of radioactive decays exist. *Alpha decay* is accompanied by the release of an alpha particle consisting of 2 protons and 2 neutrons. *Beta–decay* is realised by the emission of a beta particle identical to a negatively charged electron. *Beta+ decay*, which is less frequent, is accompanied by the emission of a positively charged positron. Electron capture occurs through the absorption of an orbital electron of an atom by the atomic nucleus. The replacement of the vacant electron position is followed by the emission of characteristic radiation (electromagnetic radiation of low energy).

Spontaneous fission occurs through the splitting of heavy atoms into two fragments and the subsequent release of neutrons and energy. The decay of a radionuclide usually leaves the newly formed nucleus in an energy excited state, and the surplus energy is radiated as gamma rays (Anon., 2003).

Radioactive decay also often occurs in a series (or chain) with a number of daughter products, which are also radioactive, and terminates in a stable isotope. In a closed system and starting with a specified amount of a mother element, the number of atoms of daughter elements and their activity grows gradually until radioactive equilibrium of the disintegration series is reached. At this point, the activities of all the radionuclides of the series are identical. Thus, the measurement of the concentration of any daughter element can be used to estimate the concentration of any other element in the decay series.

Though many naturally occurring elements have radioactive isotopes, only potassium, and the uranium and thorium decay series, have radioisotopes that produce gamma rays of sufficient energy and intensity to be measured by gamma ray spectrometry. This is because they are relatively abundant in the natural environment. Average crustal abundances of these elements quoted in the literature are in the range 2-2.5% K, 2-3 ppm U and 8-12 ppm Th.

Gamma radiation is used in geophysical radiometry due to its larger penetration depth, compared with alpha and beta radiations (Gabor and Peter, 2011)

3.2.3 Sources of Radiation

The source of gamma radiation can be natural or artificial. The natural gamma radiation that is measured, emanates from many rock types, those containing uranium and

potassium being most active including granites, shales and clays, and from radon gas in the atmosphere as a by-product of uranium. Also, cosmic radiation forms a 'background' level. Artificial sources include detecting leakage from reactors and isotopes used as tracers. These generally have much higher energy levels than natural sources.

Each gamma ray photon has a discreet energy, and this energy is characteristic of the source isotope. This forms the basis of gamma ray spectrometry – by measuring the energies of gamma ray photons, we can determine the source of the radiation. Figure 3.7 shows a typical gamma ray spectrum

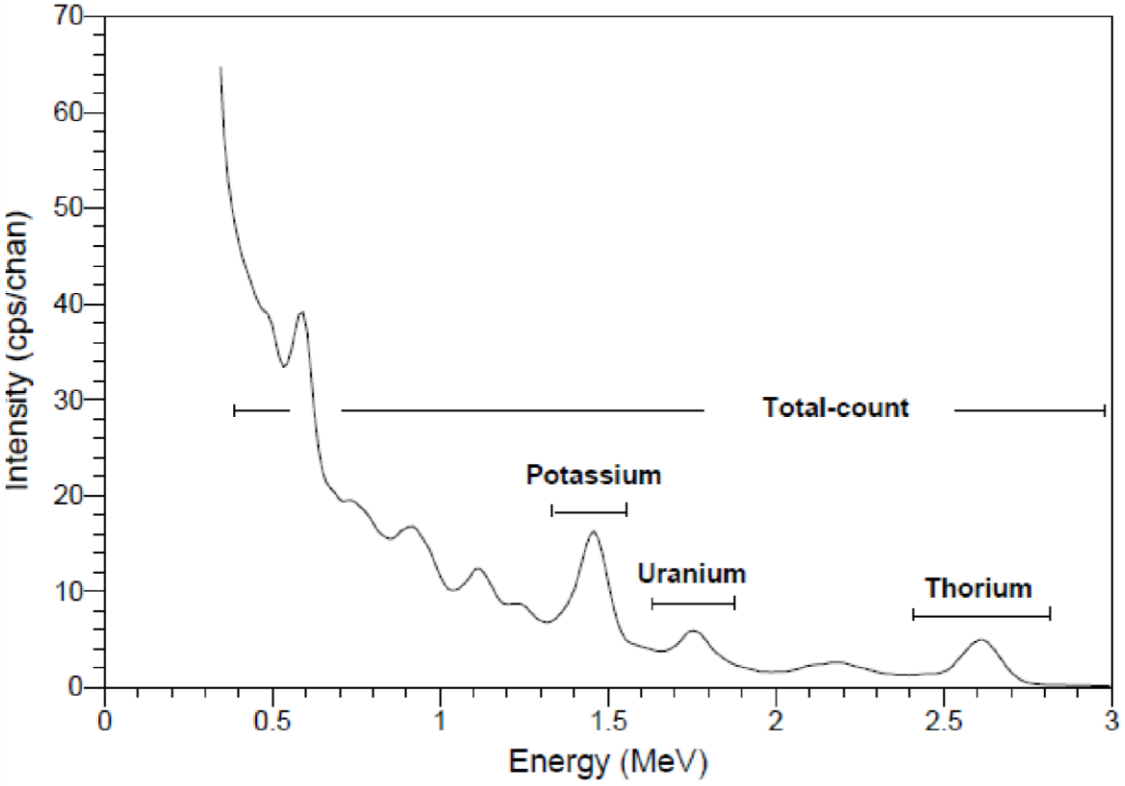

Figure 3.7 Typical Gamma Ray Spectrum Showing Positions of the Conventional Energy Windows

3.2.4 Quantities and Units

Physical quantities in atomic and nuclear physics are defined and expressed in units that have been adopted by the International Organisation for Standardization (ISO), and are described in Anon. (1992a) and Anon. (1992b). Further references for quantities and units are recent publications of the International Commission on Radiological Protection (Anon., 1991, 1993) and the United Nations Scientific Committee on Effects of Atomic Radiation. Apart from the SI units of nuclear physics, other units in common use in the

field of radioactivity and the environment can be found in Anon. (1979) and Anon. (1989). This section describes a selection of SI and conventional units in common use in these fields.

In geology and nuclear geophysics, radioelement concentrations in rocks, air and water are expressed in the following units:

mass concentration of K:	% K	(percent potassium)
mass concentration of U:	ppm U	(parts per million of uranium)
mass concentration of Th:	ppm Th	(parts per million of thorium)

1 ppm = 10^{-6} g/g = 1g/ton

Activity concentration of Rn in soil gas and air: kBq/m^3, Bq/m^3 activity concentration of radioelements in groundwater: Bq/litre, Bq/m^3

Table 3.2 shows SI derived quantities and units of radioactivity.

Table 3.2 SI Derived Quantities and Units of Radioactivity

Quantity	Symbol	Unit	Dimension	Use/Conversion of older units
Activity	A	Becquerel (Bq)	s^{-1}	radioactivity of objects
Specific activity	a	becquerel per kilogram (Bq/kg)	$kg^{-1}s^{-1}$	radioactivity of unit mass
Activity concentration	c_A	becquerel per metre cubed (Bq/m^3)	$m^{-3}s^{-1}$	radioactivity of gases and liquids
Surface activity	a_s	becquerel per metre squared (Bq/m^2)	$m^{-2}s^{-1}$	radioactivity of unit area
Exposure	X	coulomb per kilogram (C/kg)	$kg^{-1}sA$	ionizing effect of X and gamma rays in air
Exposure rate	X´	ampere per kilogram (A/kg)	$A\ kg^{-1}$	exposure per unit time, gamma radiation field. $1\mu R/h=7.17x10^{-14}A/kg$
Dose	D	Gray (Gy)	m^2s^{-2}	absorbed dose. 1 $rad=10^{-2}Gy$. $1R=8.69x10^{-3}Gy$ (in air)
Dose rate	D´	gray per second (Gy/s)	m^2s^{-3}	gamma radiation field. 1 μR/h=8.69 nGy/h in air.
Dose equivalent	H	Sievert (Sv)	m^2s^{-2}	biological effects of radiation. 1 $rem=10^{-2}$ Sv
Photon dose equivalent rate	$H´_x$	Sievert per second (Sv/s)	m^2s^{-3}	dose equivalent per unit time
Equivalent dose	H_T	Sievert (Sv)	m^2s^{-2}	biological effects of radiation
Effective dose	E	Sievert (Sv)	m^2s^{-2}	biological effects of radiation to man

3.2.5 Detectors and Instruments

The radiometric instrument measures the level of gamma radiation by recording the flashes of light, or 'scintillations' that occur when a gamma ray impinges on a special crystal called, a "phosphor". The brilliance of the flash is proportional to the gamma ray's energy and each scintillation is detected by a photomultiplier tube that converts the light into a voltage pulse. Since the value of voltage is directly related to the energy, a "spectrum' of energy levels can be developed and particular elements distinguished.

Ionization chambers, proportional counters, Geiger-Muller tubes, scintillation counters, semiconductor detectors, thermoluminiscence detectors and various mechanical and chemical track detectors are used to monitor and quantify the α, β, γ and neutron radiation of the environment. The nature and character of the radiation governs the selection of a suitable detector. The efficiency of a detector is a measure of the probability that an incident photon will be absorbed in the detector. It is usually quoted as the ratio of recorded counts to incident photons. The energy resolution of a detector is a measure of its ability to distinguish between two gamma rays of only slightly different energies. This is usually defined as the full width of a photopeak at half the maximum amplitude (FWHM) divided by its energy. Instruments used in in-situ gamma ray spectrometry are usually specified by the energy resolution of the 137Cs photopeak at 662 keV. Dead time refers to the finite time required for a detector to process an individual particle of radiation. During this time all incoming pulses are ignored. Dead time should thus be as small as possible. Few radiometric instruments are discussed.

Geiger Muller Counter

A Geiger-Muller counter (GM counter) consists of a gas-filled tube equipped with a metal cylinder (the cathode) and a thin conductive wire (the anode) mounted along the tube axis. Normally argon, with an admixture of halogen vapour, is used as gas filling. GM counters are 2 to 30 cm long and 1 to 4 cm in diameter, and they operate with applied voltage of several hundred volts. GM counters make use of the progressive growth of ionization in a strong electric field between the anode and the cathode. An incident photon interacts with the cathode and releases an electron that may be directed into the GM tube. The growth of ionization between the anode and the cathode amplifies the signal and generates an electric current between the electrodes. This results in a voltage pulse at the anode output of the GM counter. The multiplication coefficient of the gas ionizing chain reaction is of the

order of 10^6, and the output pulse is not proportional to the absorbed gamma ray energy. The detection efficiency of GM counters is very low (less than 2%) and the dead time is of the order 10^{-4} s. Figure 3.8 is a picture of a Geiger Muller counter.

Figure 3.8 Geiger Muller Counter

Gamma Ray Spectrometer

Gamma ray spectrometers use the direct proportionality between the energy of an incoming gamma ray and the pulse amplitude at the output of the detector. Figure 3.9 shows a block diagram of a gamma ray spectrometer. After amplification and digitisation, the pulse amplitudes are analysed, and the output of the spectrometer is an energy spectrum of detected radiation. Since individual radionuclides emit specific gamma ray energies, gamma ray spectra can be used to diagnose the source of the radiation.

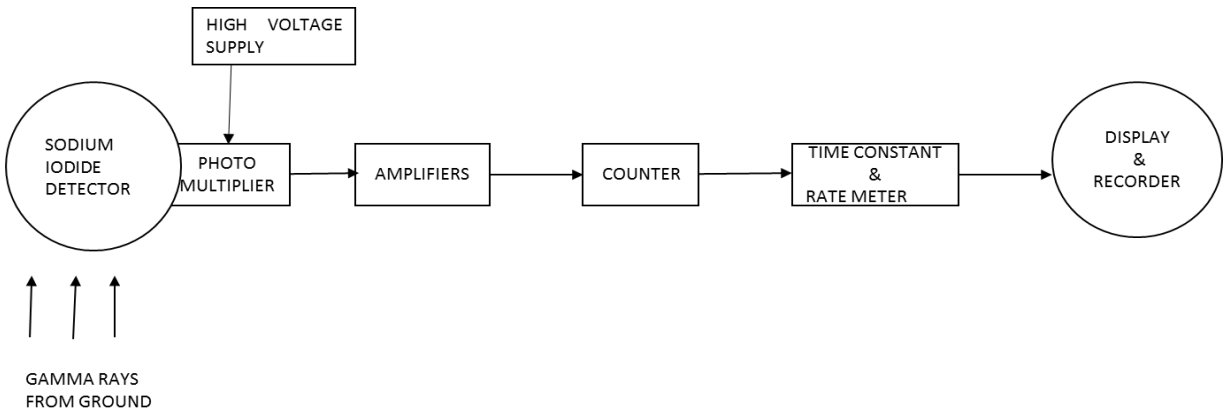

Figure 3.9 Block Diagram of a Gamma Ray Spectrometer

Gamma ray spectrometers are either “integral” or “differential”. Integral spectrometers record only those pulses with amplitudes exceeding a discrimination threshold. This threshold can be changed to allow the discrimination of individual radionuclides. Differential gamma ray spectrometers record pulses whose amplitudes fall within a given amplitude interval (or channel), corresponding to a discrete range of gamma ray energy. Wider energy intervals (comprising several channels) are called energy windows. Modern analysers use as many as 256 or 512 channels, with a width of several keV per channel. Older systems are limited to recording several distinct energy windows. Gamma ray spectrometers should have amplitude gain stabilization to avoid the effect of energy spectrum drift. Gain stabilization can be accomplished by controlling the temperature of the detector, or by spectrum energy stabilization using either a reference radioactive source or the measured spectrum. Figure 3.10 is a picture of a Gamma Ray Spectrometer.

Figure 3.10 Gamma Ray Spectrometer

Scintillation Counter (Scintillometer)

Scintillation counters consist of a scintillator and a photomultiplier. An incident gamma ray photon interacts with the material of the scintillation crystal to produce scintillations. These photons of visible light induce the ejection of electrons from the photocathode of the attached photomultiplier. Their number multiplies progressively at dynodes of the photomultiplier, and an electron cloud strikes the anode. This induces a negative voltage pulse as output, with amplitude proportional to the energy of the incident photon. Scintillation counters are widely used in gamma ray spectrometry. Thallium-activated

sodium iodide NaI (Tl) crystals are mainly used as detectors in field gamma ray surveys. They are transparent, with a high density (3.66 g/cm), and can be manufactured in large volumes. They have a detection efficiency of up to 100% for low-energy gamma rays but somewhat less for high-energy gamma rays. The dead time is of the order 10^{-7} s and the energy resolution for 137Cs at 662 keV is in the range ranges 7-10%, depending on the volume and quality of the detector. NaI (Tl) detectors are hygroscopic, they age, they are fragile, and the photomultiplier tube function is dependent on temperature. Their large crystal volumes are an advantage in applications such as airborne surveying where measurement times are necessarily short. Thallium-activated caesium-iodide CsI (Tl) crystals are neither hygroscopic nor particularly fragile. They have a density of 4.51 g/cm3, and a dead time of the order 10^{-9} s. But they are too expensive for widespread use. Plastic scintillators are an admixture of a scintillator and a plastic transparent material. They can be produced in large volumes but have poor energy resolution and are not suitable for gamma ray spectrometry. Figure 3.11 shows a picture of a Scintillation Counter.

Figure 3.11 ECL Model 9 “Crysto Count” Scintillation Counter

Germanium Semiconductor Detectors

Germanium semiconductor detectors use the electronic carriers (electron-ion and electron-hole pairs) created by the absorption of gamma ray photons in the germanium detector. These collect directly on the detector electrodes, causing a flow of electric current through the semiconductor and produce an output voltage pulse of amplitude proportional to the energy of the incident gamma ray photon. The detector consists of a germanium crystal mounted in a vacuum cryostat cooled to -196 °C. Cooling is by insertion of the cryostat in a dewar vessel filled with liquid nitrogen, or by electrically powered cryogenic refrigerators. The detectors are generally of small volume and used in in-situ gamma ray spectrometry. The energy resolution of these detectors is very high, but because of their small volume, their sensitivity is low and it may take tens of minutes to record a spectrum (Figure 3.12).

Figure 3.12 A Germanium Semiconductor Detector

3.2.6 Use of Radiometric Survey in Mineral Exploration

Coker *et al.* (2013) used radiometric survey to successfully delineate between sedimentary terrain and basement complex in South-western Nigeria. Also, drill targets were delineated at RCU and HPU Properties located in the Sudbury Mining District of northern Ontario, Canada, using detailed ground radiometric survey (Anon., 2009).

Wemegah *et al.* (2015) used airborne magnetic and radiometric datasets to interpret the geology and geological structural patterns which serve as potential gold mineralisation zones in the Cherano area located at south-western boundary of the prospective Sefwi Gold Belt and the Kumasi Basin in southwestern Ghana.

CHAPTER 4

METHODS USED

4.1 Source of Data Used

Magnetic susceptibility, radiation, lithological and multi-element assay data of core samples from thirty-seven (37) HQ size diamond drilled holes of about 9200 m were used for analysis. Geophysical data were collected within the period August 2010 and March 2013. Standard procedures and protocols were at all times adhered to as illustrated in this chapter.

4.2 Field Equipment

The equipment used for the data collection include the SM30 magnetic susceptibility meter and SPP2 NF Scintillometer. Both instruments were obtained from Burey Gold ltd.

4.2.1 The SM-30 Pocket Size Magnetic Susceptibility Meter

The SM-30 was used to measure the magnetic susceptibility of the drill core. This instrument was chosen because of its portability, high sensitivity, low noise, deep penetration and simple operation. Also, the instrument output does not include any correction for sample volume or mass. It is an accurate tool for field measurement of susceptibility of outcropping rocks, drill cores or rock chips.

The SM-30 is controlled by three push buttons. If no button is pressed for 3 minutes, the instrument switches off automatically. It has a beeper indicating intervals in which the information from the rock is picked-up. The SM-30 is powered from two coin-sized lithium batteries CR2430.

This instrument offers six measuring modes. Two of them are basic, two compensate the linear part of the thermal drift, one is for scanning (e.g. drill core scanning), and one is for averaging. The large number of the memory registers (250) is useful especially when scanning mode is used. Though the instrument is small, the pick-up coil is large enough in diameter to measure sufficiently high volume.

An interpolation method was used for the SM-30 measurements, whereby a free-air measurement is taken, followed by a direct measurement on a drill core, and finally a second free-air measurement, where the first and third measurements are compensation steps.

4.2.2 Magnetic Susceptibility Data Collection

The magnetic susceptibility readings were taken at 20 cm (0.2 m) intervals. The procedure involved the following;

i. 20 cm marks were drawn on the core,
ii. The core was placed in an area clear of all metallic influence,
iii. The piece of core to be measured was places on a wooden board devoid of any metallic influence,
iv. The SM30 was first used to take free-air measurement by holding it facing open air and pressing the measure button until the beeper sounds to indicate reading has been taken,
v. Then holding the instrument in contact with the core surface the measure button was pressed again until the beeper sounded indicating measurement had been taken,
vi. The measured magnetic susceptibility is read from the electronic display of the SM30,
vii. The magnetic susceptibility value k1 is recorded on a magnetic susceptibility log sheet,
viii. The process is repeated on the same meter and a second magnetic susceptibility value k2 for the metre recorded,
ix. The magnetic susceptibility for the metre kM is the average of k1 and k2
x. Figure 4.1 is a photograph of the author taking magnetic susceptibility of drillcore using the SM-30 meter.

Figure 4.1 Magnetic Susceptibility Data Collection with SM-30

Strict field and operational rules were kept throughout the period in order to obtain good result and protect the instrument against damages. These are as follows:

i. Do not measure with weak batteries (change batteries after Low Battery signal appears).
ii. Do not measure in the rain when the surfaces of drillcore are very wet
iii. Do not wear rings, metallic watches and other ornaments when taking readings
iv. Broken core must be rearranged as much as possible to its cylindrical shape
v. Free-air measurement should not be executed near metallic earrings, necklaces or any other metallic objects, but in the free air, at least 50 cm in distance from them
vi. When measuring the drillcore, avoid measuring near the nails of wooden core boxes. Never measure cores placed in metallic boxes. The best way is to take cores from the box away from metallic objects
vii. When putting the instrument on rock surface, make it gently, beware shocks and pressing on the coil, because it can be damaged by rough handling

4.2.3 The SPP2 NF Scintillometer

Drill core radiometry was done using the Saphymo-SRAT SPP2 NF Scintillometer. It is manufactured by Saphymo-PHY (Massy, France) and is designed for uranium exploration in rugged conditions. The detector is 1 X 1.5 inch (15.3cm^3) NaI(Tl) (Sodium Iodide activated with Thallium) scintillation crystal. The operation range for gamma radiation is 0.02 to 30 microsieverts per hour (µSv/h). The instrument has an in-built audible alarm that gives a high signal. The threshold and the frequency of the sound alarm can be varied according to the strength of radiation. The time constant for the sound alarm is 0.25 seconds. The SRAT's unit of measurement is cps (counts per second). It is 32 X 13 X 12 cm in size and weighs 3.6kg.

The SPP2 NF is a γ and X Portable Prospecting Scintillometer specially designed for on field use in extremely harsh environment. The SPP2 NF is intended to detect radioactivity and gamma –X radiation whose energy exceeds 30keV. The instrument is gun type handled and connected by cable to an electronic box which can be clipped to a belt for carrying. The box includes all the electronics, power supply and audible alarm.

The SPP2 NF is a precision instrument for tracking radioactive sources and materials. It can be used under harsh conditions. For these reasons, it is used by a large variety of operating teams, from Emergency Fire Response to Uranium Prospection.

Figure 4.2 The SPP2 NF Scintillometer

4.2.4 Drillcore Radiometric Data Collection with the SPP2 NF Scintillometer

Taking the drillcore radiometric readings involved the following steps:

i. Drillcore was arranged on V-shaped metal core racks separated by at least 3m from each other to prevent cross-over radiation influences.
ii. 10cm interval marks were marked on the core
iii. The Scintillometer is held 10cm directly above the core
iv. The control is set to 150R, which can measure radiations up to 150cps (counts per second)
v. If the radiation coming from the core is less than 150cps, the maximum and minimum values are read from the counter and recorded
vi. But if the radiation is greater than 150cps, the inbuilt alarm goes off and the counter reads the maximum value of 150 cps. The control is then reset to 500, and the count rate recorded
vii. The Control is calibrated in 150R, 150L, 500, 1500, 5000 and 15000. The instrument can measure up to 15000cps of radiation
viii. The average value for the maximum and minimum readings is calculated as the radiation at the point.

Precautionary measures taken to ensure accurate radiation measurement include;

i. The scintillometer should be held directly above the core, to ensure that atmospheric radiation is minimised
ii. The clearance between the scintillometer and the core should be 10cm, this ensures that only radiation coming from the marked 10cm is being picked up by the scintillometer
iii. The location for taking the readings should be free of radiometric anomalies or substances
iv. The average time for taking readings was 30 seconds. This allows accurate readings to be taken for a substantial length of core over a short period
v. The fast response of the Scintillometer and the frequency modulated audible signal makes it easy for anomalous zones to be easily picked up.

.

4.3 Laboratory Assay

After radiometric and magnetic susceptibility information were taken, the drill core was marked for sampling taking into consideration lithological and structural boundaries. The core was split into equal halves using the core splitter. Half core samples were taken and processed for submission to the laboratory for assay.

Samples were transported to the laboratory for analysis. Samples from the Central Polymetallic Prospect (CPP) were analysed for Gold whilst multi-element analysis was carried out for samples from anomaly E and other areas.

Assay turnaround time had been a challenge for the Balatindi Project since it took three months before assay results were received coupled with the cost of transportation.

4.4 Data Processing

The SM-30 is calibrated in X 10^{-3} from factory and therefore, values of magnetic susceptibility read off the equipment are multiplied by 10^{-3} to give the true magnetic susceptibility value.

The magnetic susceptibility data was taken at 2cm interval, the radiometric readings were taken at 1cm interval whilst laboratory assay samples were taken at least 50cm and at most 200cm depending of the geology and structure of the interval.

In order to carry out the comparative analysis required in this project, the gold assay values were composited at 2cm interval whilst assay values for uranium were composited at 1cm interval. Compositing allows effective use of observational and statistical methods to do comparative analysis.

Sample interval that had no magnetic susceptibility or radiometric readings taken were not included in the analysis.

CHAPTER 5

RESULTS AND DISCUSSIONS

5.1 Field Data and Assay Results

Magnetic susceptibility data were obtained for the 13 drillholes located within the Central Polymetallic Prospect (CPP) area, whiles radiometric data were taken for the 23 drillholes in areas A to E. These data were correlated with the laboratory assay results for gold and uranium respectively.

Strip logs comprising trace shades, histograms and line graphs were used for the interpretation with trace shades representing lithology, histograms representing laboratory assay results for gold and uranium, and line graphs representing magnetic susceptibility and radiometric readings.

5.2 Magnetic Susceptibility

The SM30 magnetic susceptibility meter read in 10^{-3} units, thus values read from the meter are multiplied by 10^{-3}. The minimum and maximum susceptibility values recorded were -2.46 X 10^{-3} and 546.5 X 10^{-3} respectively. An average of 12.575 X 10^{-3} susceptibility value was determined from the values recorded.

The various mineralised and non-mineralised rock units gave varied magnetic susceptibility values.

5.2.1 Quartz Monzonite

These units occurred as quartz-phyric dykes in the granitoids and other units. They were generally less mineralised with sizes ranging between veinlet to 15 m wide. These dykes exhibited a low magnetic susceptibility, even though elevated values were recorded at intervals where the unit host relics of granodiorite. The recorded low magnetic susceptibility is because the dominant mineral in the unit is quartz. Quartz is diamagnetic and generally has a negative or very low magnetic susceptibility. Typical of this observations made on BLDD003 and BLDD009 are given in Figure 5.1 and Figure 5.2 respectively. Susceptibility values between 0.007 X 10^{-3} and 59.7 X 10^{-3} were recorded. An average of 7.7 X 10^{-3} magnetic susceptibility is high in absolute terms, but it is

relatively low in comparison to the 12.575 X 10^{-3} average magnetic susceptibility in the CPP area. No correlations were observed between Au and magnetic susceptibility in this unit. A scatter plot of magnetic susceptibility against gold assay values for quartz monzonite is also given in Figure 5.3. The low correlation coefficient (R^2) value of 0.003 shows that there is only a 0.3% statistical chance of a relationship between magnetic susceptibility and Au mineralisation in quartz monzonite.

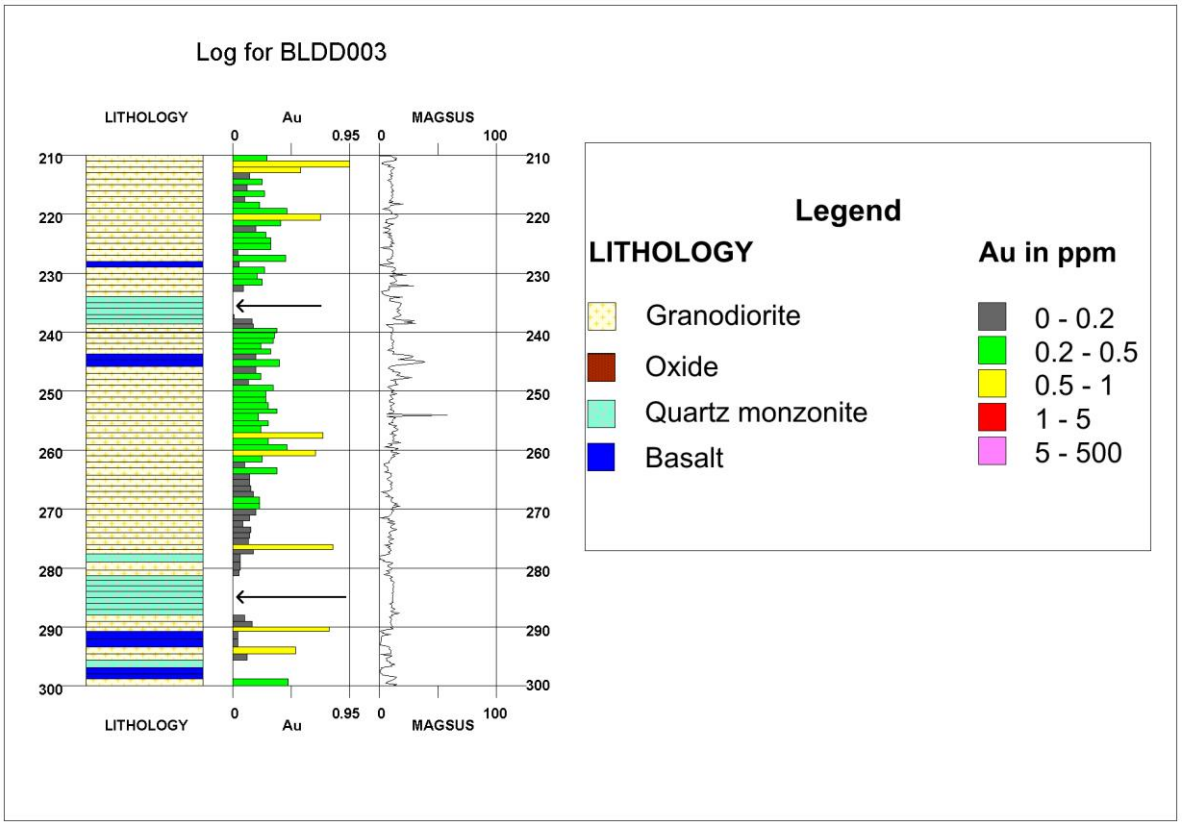

Figure 5.1 Quartz Monzonite Showing Low Magnetic Susceptibility in BLDD003

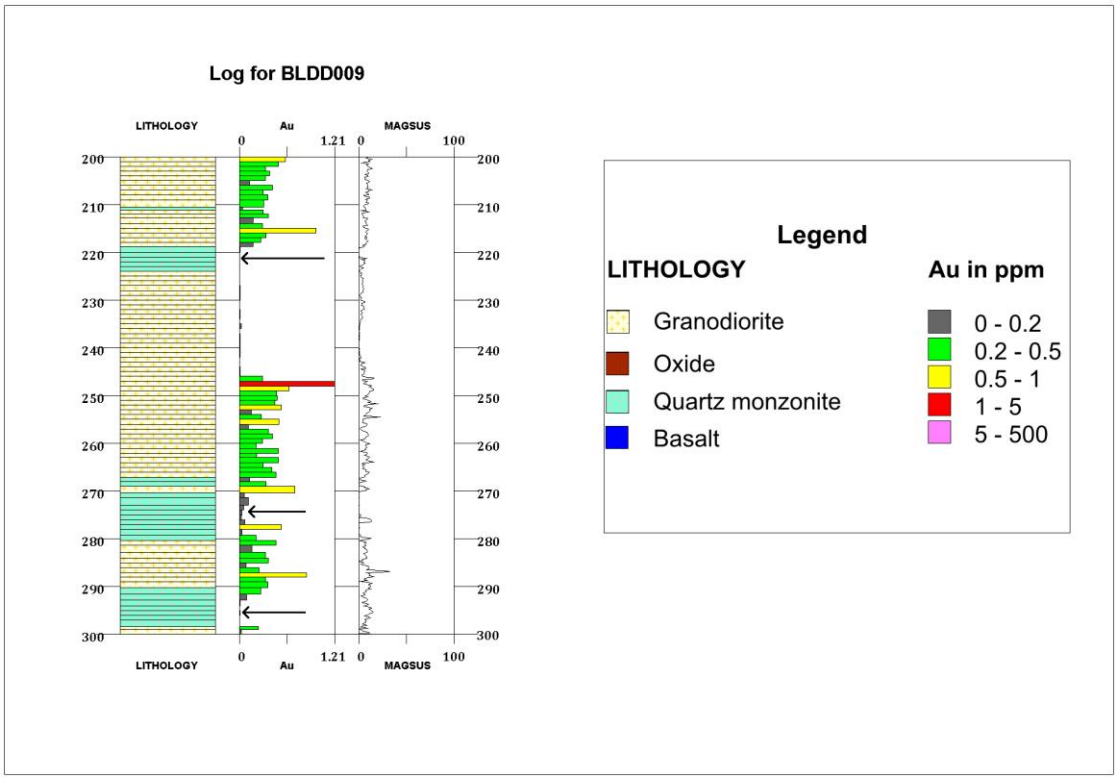

Figure 5.2 Quartz Monzonite Showing Low Magnetic Susceptibility in BLDD009

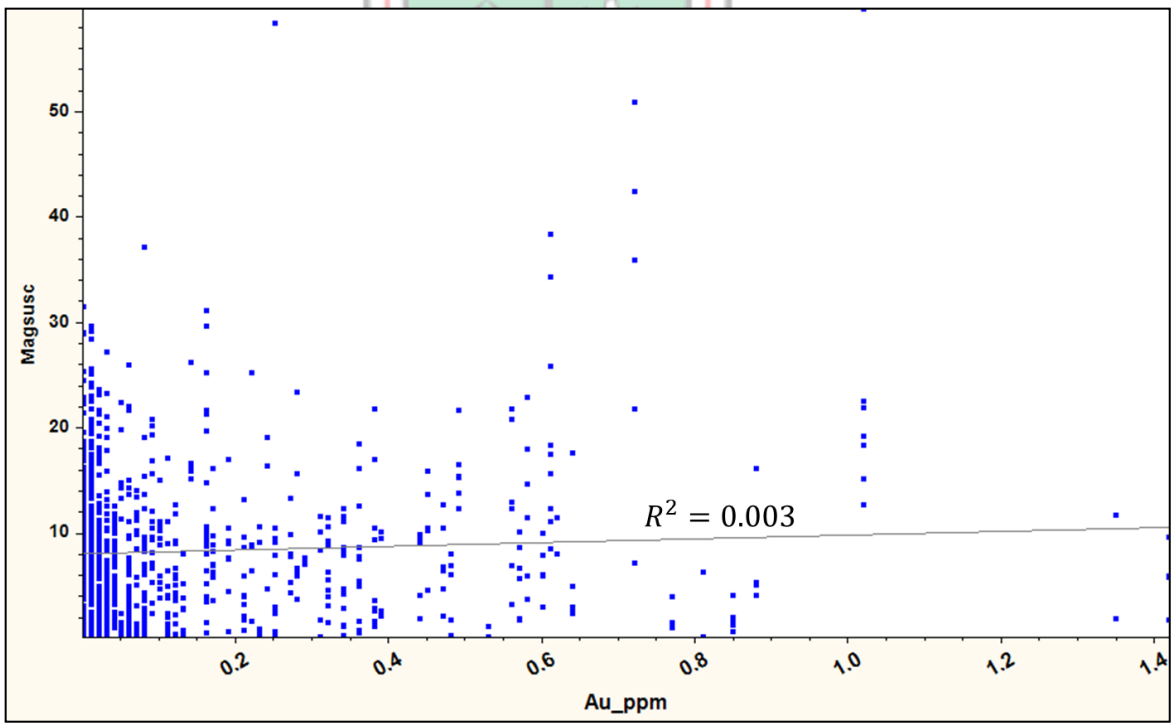

Figure 5.3 Scatter Plot of Magnetic Susceptibility against Au Assay Values for Quartz Monzonite

5.2.2 Greywacke

Greywacke encountered downhole also exhibited relatively moderate magnetic susceptibility. It occurred as massive continues unit at the bottom of BLDD006. 0.33 X 10^{-3} and 54.25 X 10^{-3} are the maximum and minimum susceptibility respectively recorded for the unit. Gold mineralisation is also restricted to zones with quartz veins and relics of granodiorite and shows no correlation with magnetic susceptibility as shown in Figure 5.4.

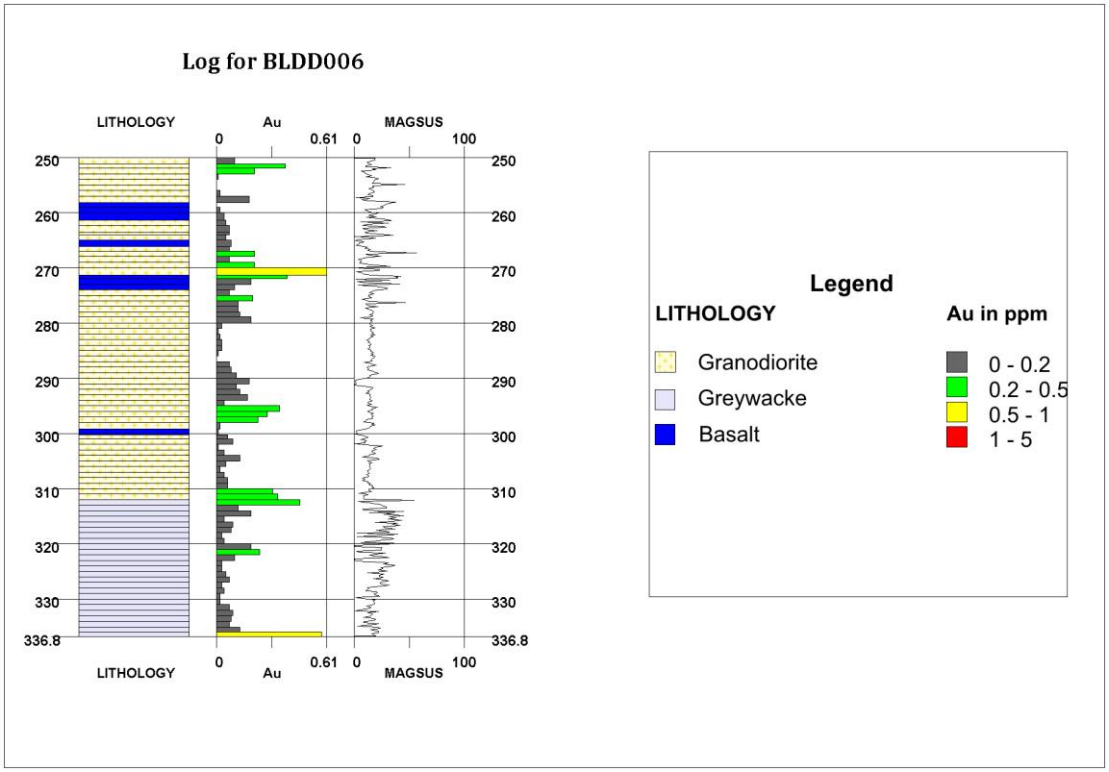

Figure 5.4 Greywacke Showing Low Au and Varied Mag. Sus. Values in BLDD006

5.2.3 Basalt

Maximum and minimum susceptibility values of 166.45 X 10^{-3} and 0.04 X 10^{-3} were recorded for basaltic units. The average value of 18.3 X 10^{-3} is the highest for a rock unit in the CPP area. Gold values were generally low and unrelated to the magnetic susceptibility values. Figure 5.5 shows areas of high magnetic susceptibility with low Au anomalies in BLDD035 while Figure 5.6 shows a scatter plot of all magnetic susceptibility and gold assay values for basalt.

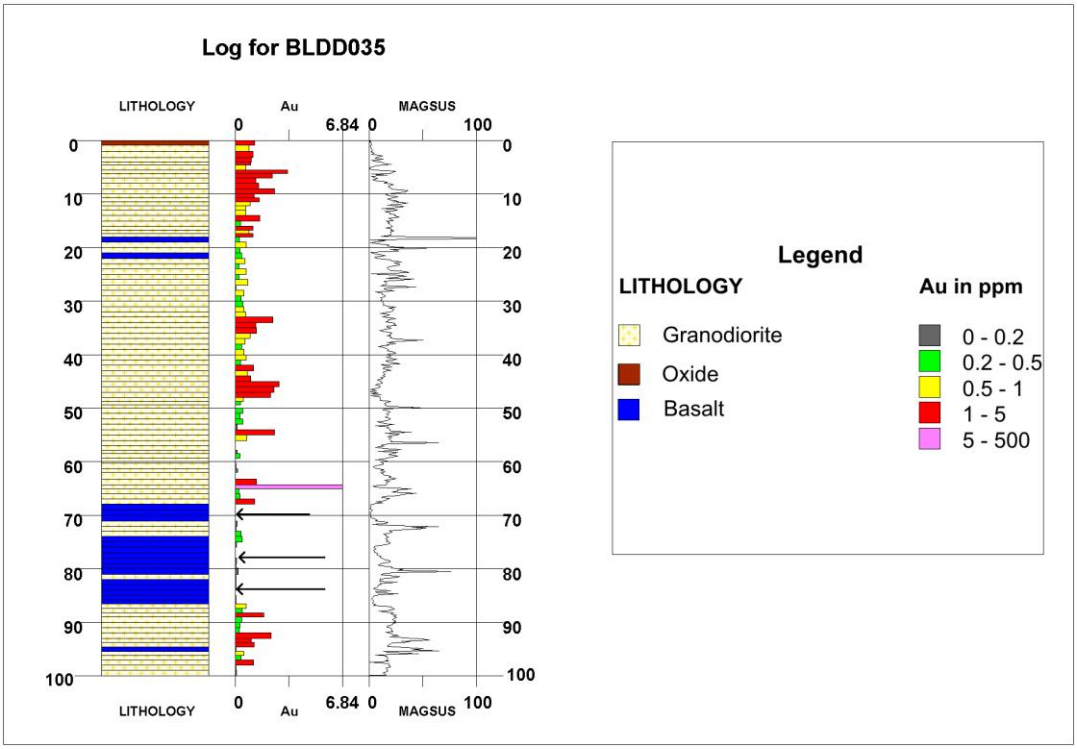

Figure 5.5 Basalt Showing Low Au Associated with High Magnetic Susceptibility in BLDD035

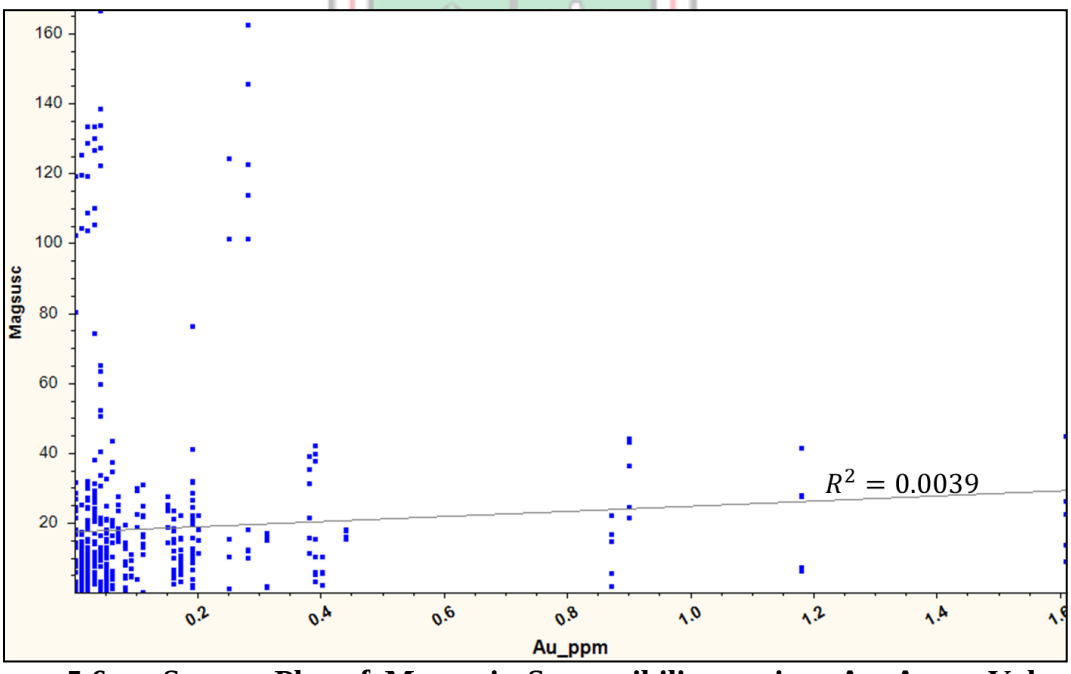

Figure 5.6 Scatter Plot of Magnetic Susceptibility against Au Assay Values for Basalt

5.2.4 Dacite

Dacite logged in BLDD007 and BLDD010 returned very low Au values. The few elevated value reported show relations to quartz veining rather than the lithological unit. An average of 10.85 X 10^{-3} magnetic susceptibility value indicates a moderately high magnetic unit. Comparison of Au assay and magnetic susceptibility values showed no correlation. Figure 5.7 and Figure 5.8 are strip logs of BLDD007 and BLDD010 showing dacite units with low magnetic susceptibility and Au values. Figure 5.9 shows a scatter plot of magnetic susceptibility against Au values for dacite unit.

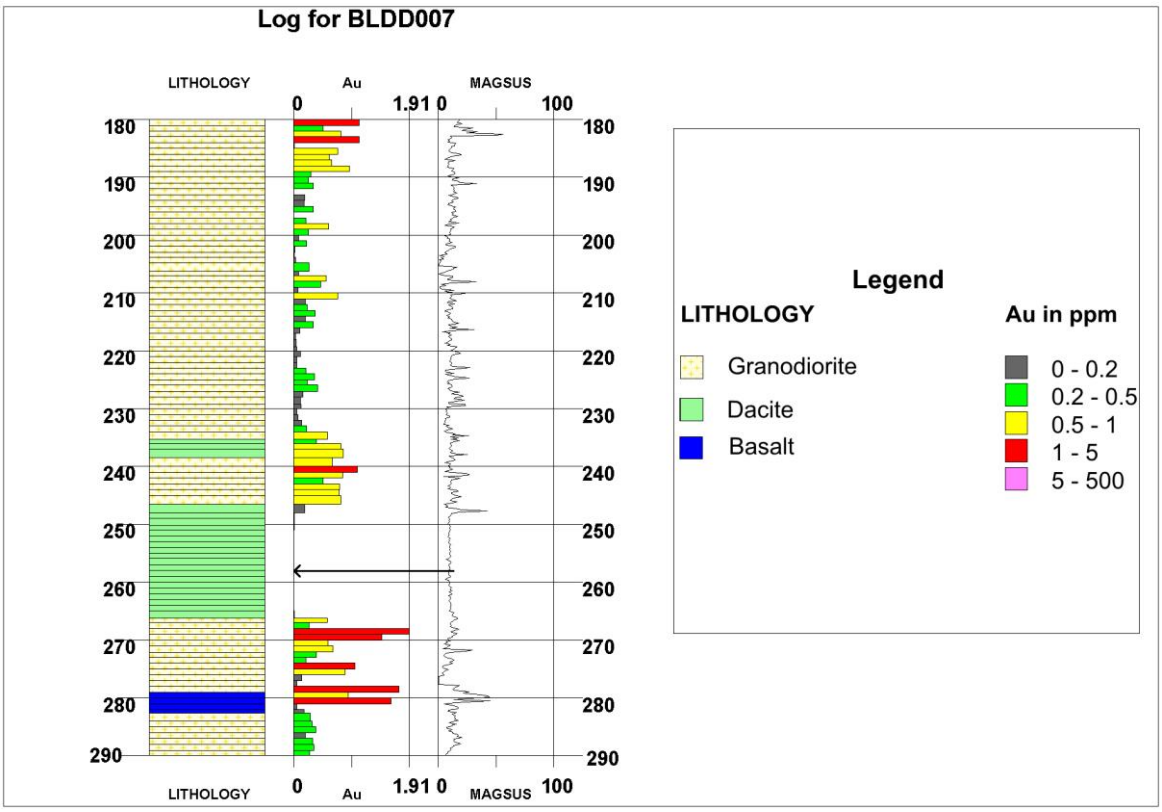

Figure 5.7 BLDD007 Showing Low Au and Low Magnetic Susceptibility in Dacite

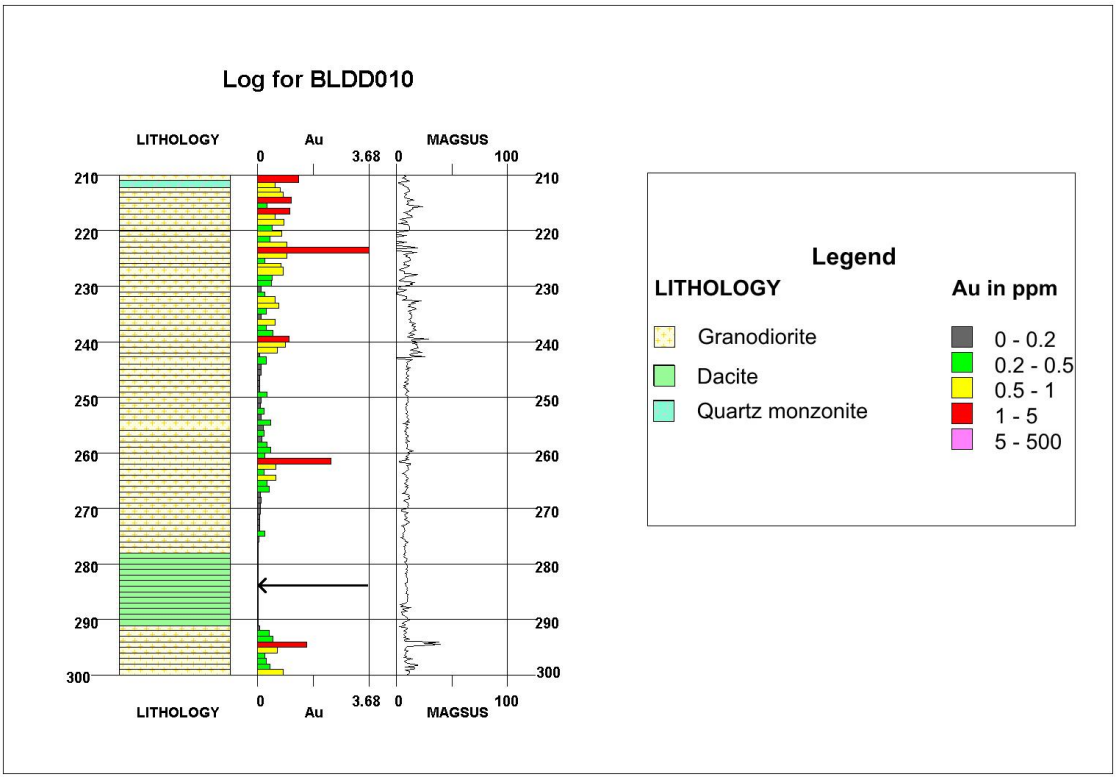

Figure 5.8 Showing Dacite Unit with Low Au and Magnetic Susceptibility in BLDD010

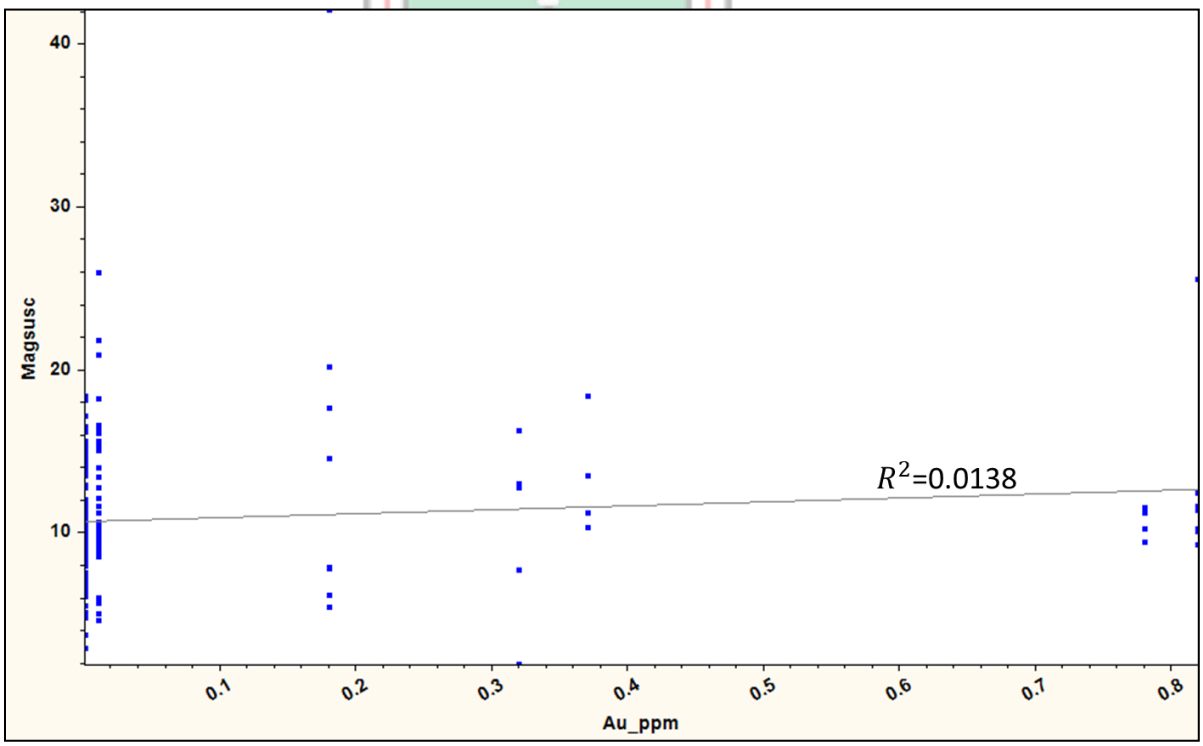

Figure 5.9 Scatter Plot of Magnetic Susceptibility Against Au Assay Values for Dacite

5.2.5 Granodiorite

The granodiorites host the Au mineralisation in the Balatindi mineral prospect. They are fine to medium grain, k-feldspathic units with magnetite bands concordant to foliation. Mineralisation occur in the form of chalcopyrite and pyrite, disseminated and along vein selvages. Figure 5.10 shows typical mineralised drill core from the Balatindi project.

Magnetic susceptibility reading in these units is wide and varied. Comparative analysis were carried out for various ranges of magnetic susceptibility and Au assay values. Observations were made for negative magnetic susceptibility, low magnetic susceptibility and high magnetic susceptibility values and the observations are discussed.

Figure 5.10 Mineralised Granodiorite in T03/14 and BLDD035

Negative Magnetic Susceptibility

Negative magnetic susceptibility values were recorded in three drill holes, BLDD005, BLDD007 and BLDD008. The lithology reveals that these negative magnetic susceptibility zone are near surface silicified or quartz vein areas. The magnetite is weathered and leached out leaving essentially quartz. All the zones with negative susceptibility returned anomalous Au assays. However, only a few negative magnetic susceptibility values were recorded and therefore a generalised conclusion cannot be drawn. Figure 5.11 shows BLDD005 showing intervals with negative magnetic susceptibility that returned strong Au anomalies.

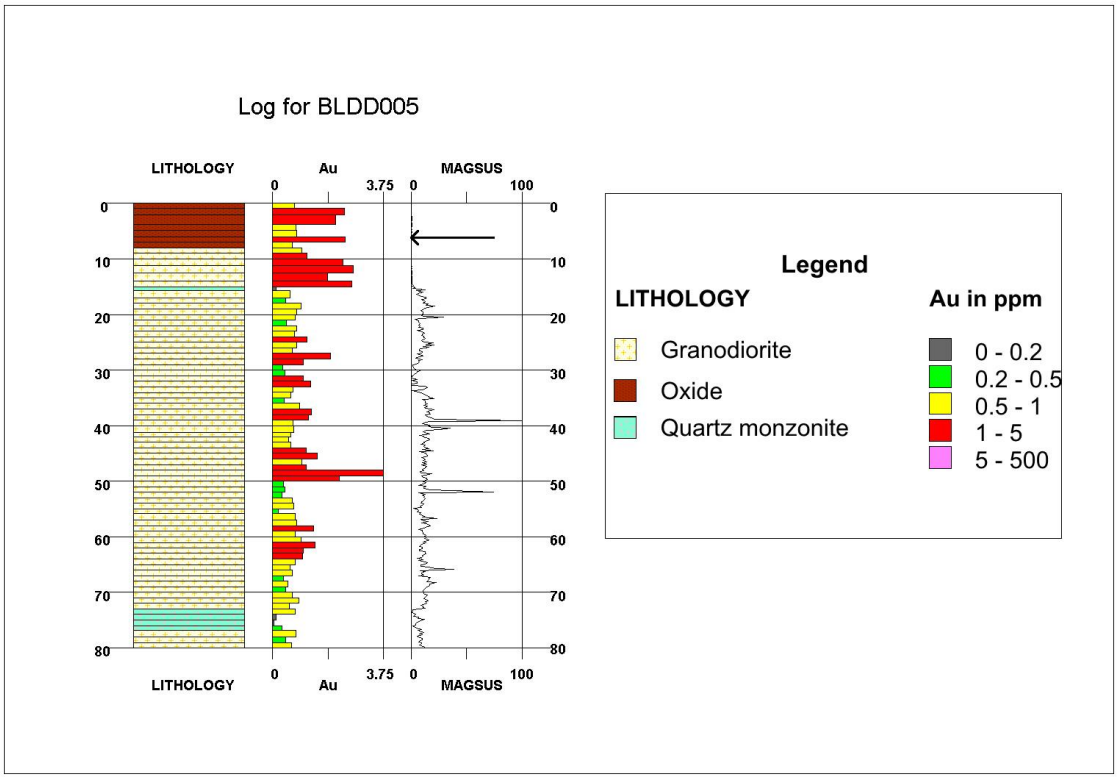

Figure 5.11 Showing Negative Magnetic Susceptibility Associated with High Au Values in BLDD005

Low Magnetic Susceptibility

Susceptibility values of between 0 and 5 X 10^{-3} are considered low in terms of the Balatindi area. Low magnetic susceptibility values correlated favourably with Au anomalies in certain intervals. This is explained by the fact that low susceptibility mark areas of silicification and quartz veining that destroys the magnetite fabric within the unit. Mineralisation within the Balatindi area is associated with silicification, quartz veins and

sulphide (chalcopyrite and pyrite) mineralisation. Figure 5.12 and Figure 5.13 show some intervals in BLDD004 and T03/17 respectively, where low magnetic susceptibility values correlated with high Au assay values.

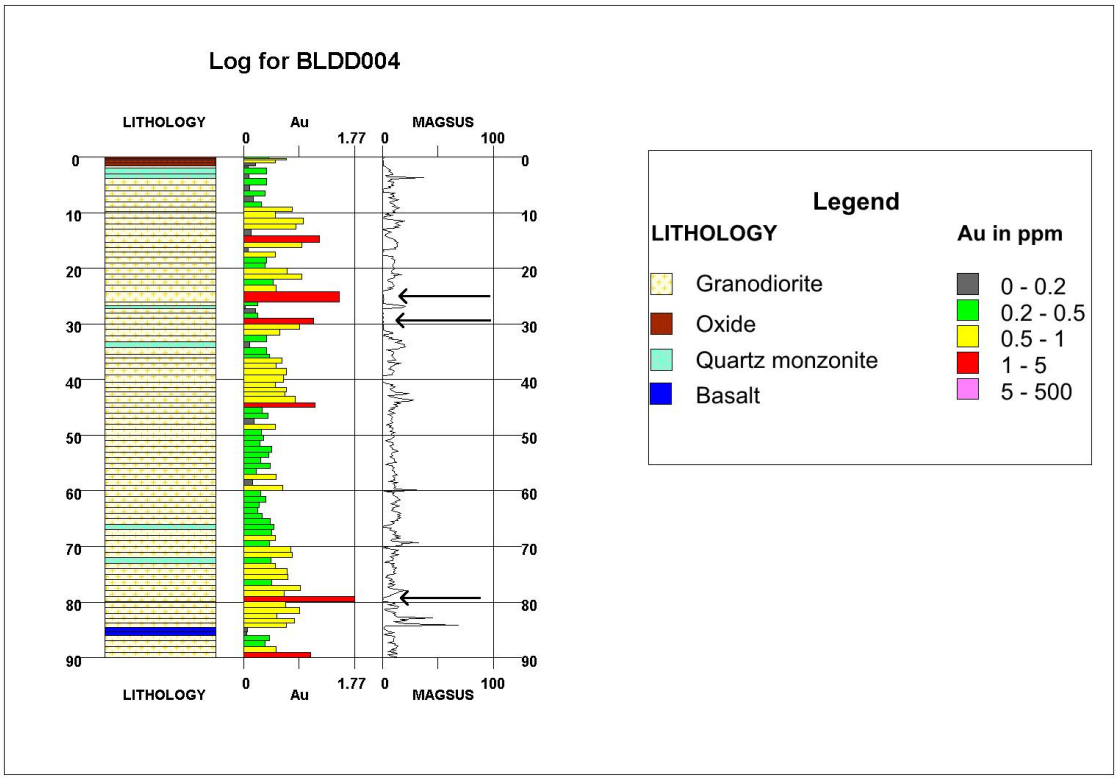

Figure 5.12 BLDD004 Showing Low Magnetic Susceptibility Associated with High Au Anomalies

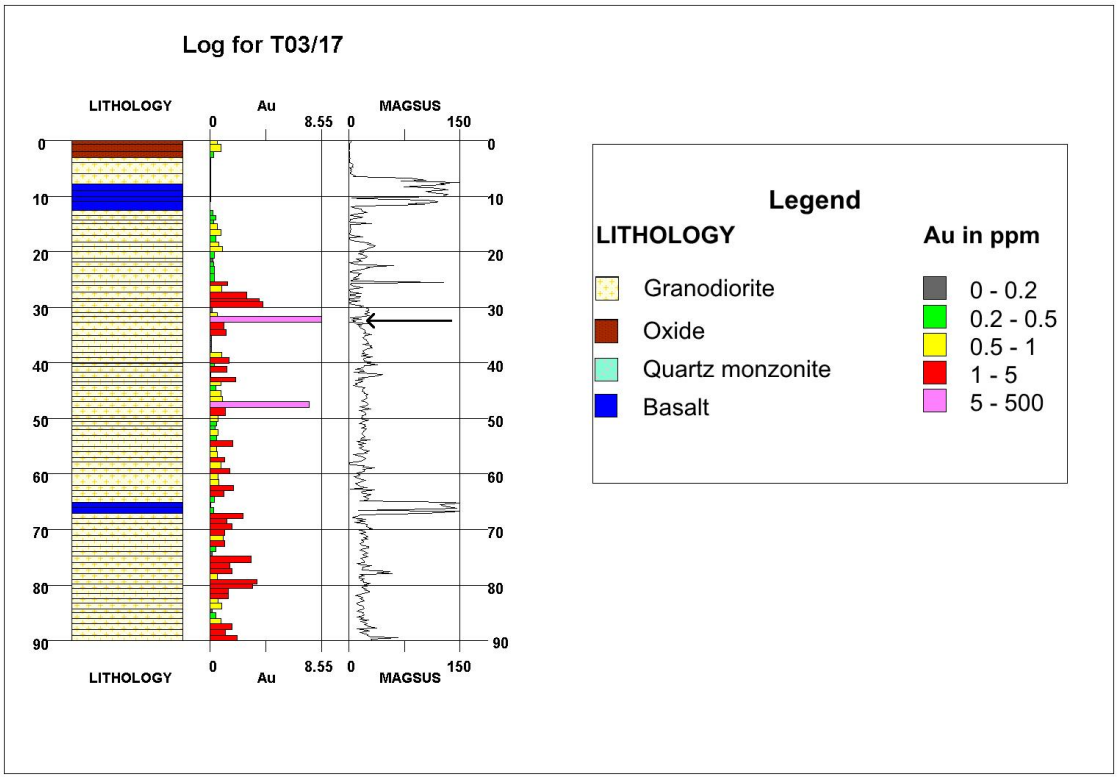

Figure 5.13 T03/17 Showing Low Magnetic Susceptibility Assoc. with High Au Assay Values

High Magnetic Susceptibility

High magnetic susceptibility area exhibit an interesting phenomenon in relation to Au mineralisation. Contrary to expectation, some areas with extremely strong magnetic susceptibility also returned high Au anomaly. Examination of lithology reveals intense foliation characterised by magnetite banding and usually with chalcopyrite or sulphide filled joints. Figures 5.14 and 5.15 show typical situations in BLDD001 and BLDD002

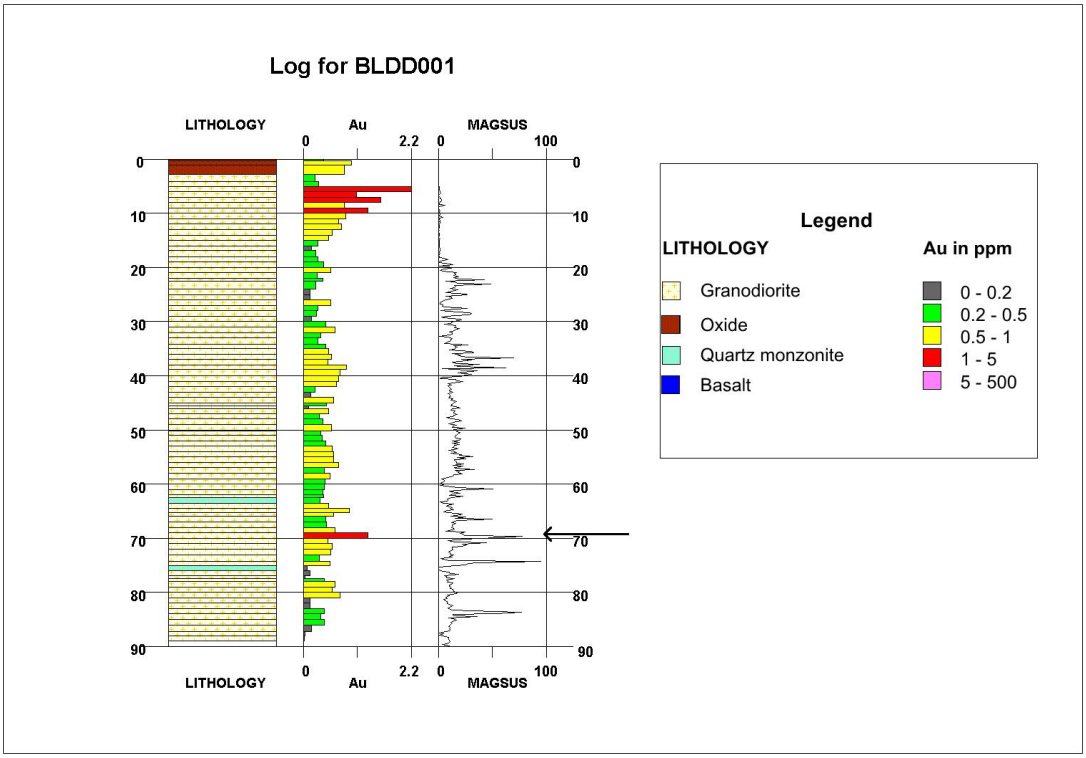

Figure 5.14 BLDD001 Showing High Magnetic Susceptibility Associated with High Au Values

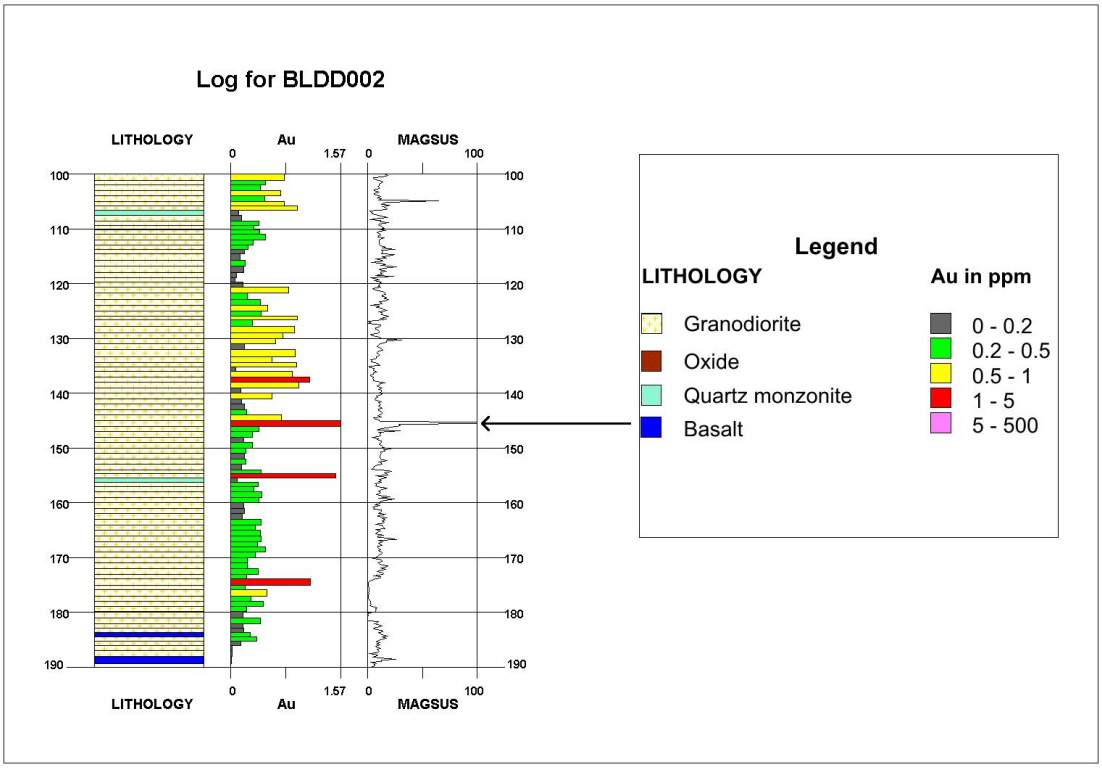

Figure 5.15 High Magnet Susceptibility Associated with High Au Assay Values in BLDD002

Statistical Comparison of Magnetic Susceptibility and *Au Mineralisation*

A statistical comparison of magnetic susceptibility readings and gold mineralisation was done for the granodiorite unit. In doing this, a scatter plot of magnetic susceptibility and Au in ppm was drawn and a correlation sought.

As can be seen from the scatter plot in Figure 5.16, a meaningful correlation could not be established between the magnetic susceptibility reading and Au assay values

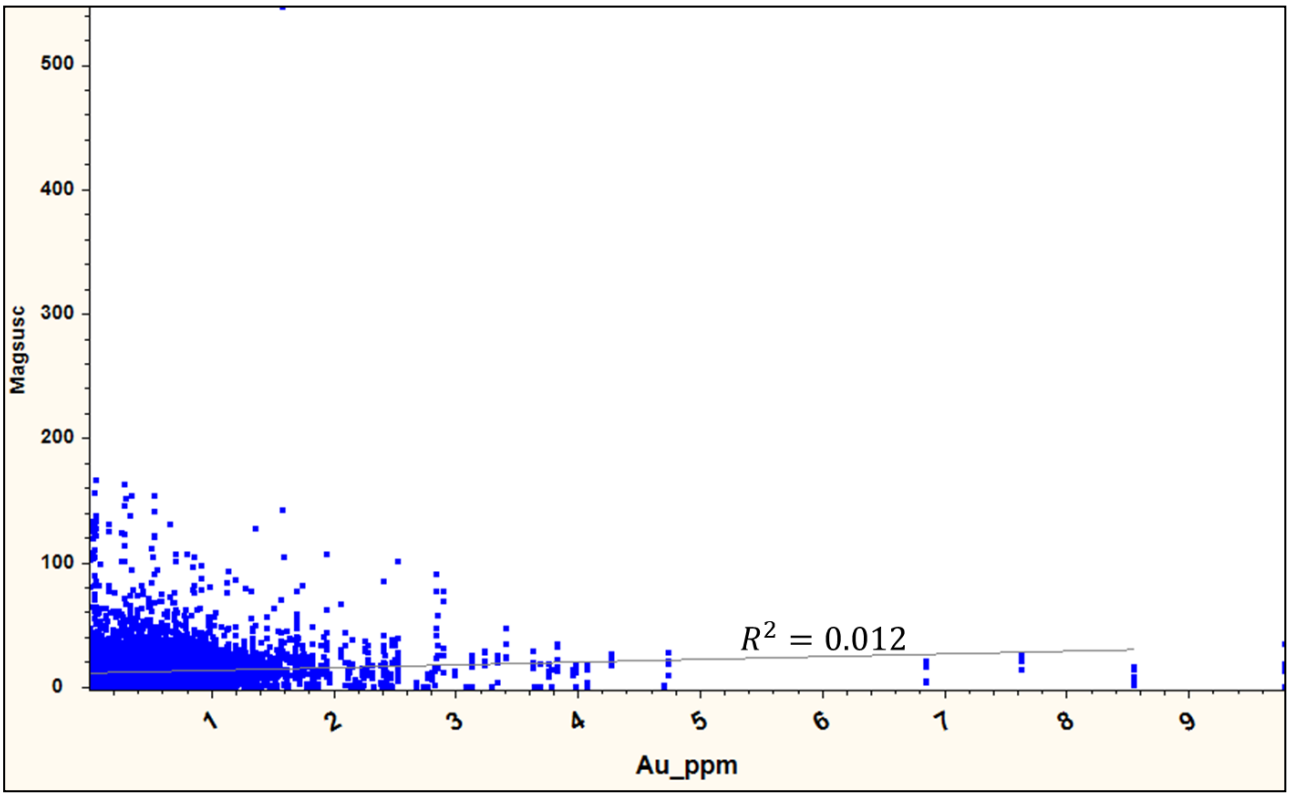

Figure 5.16 Scatter Plot of Magnetic Susceptibility vrs Au in ppm

5.3 Radiometric Readings (cps)

The SPP2 NF Scintillometer is a total counts instrument that records total radiations regardless of their source. Anomalous readings could therefore be from uranium, thorium, potassium or a combination of the three sources. 45 and 7250 cps were the maximum and minimum values respectively recorded for the radiometric readings

5.3.1 Radiation cps and Lithology

Strip logs comprising lithology, histogram and line plots of the radiometric counts per second against uranium mineralisation and the lithology reveals that, massive rock units such as basalt, intermediate volcanic and greywacke did not return anomalies for uranium. However, some fractured areas within these units showed elevated values. This is explained by the fact that uranium is highly mobile, though unable to penetrate the massive rock unit, it able to disperse through its fractures. Figure 5.17 and Figure 5.18 show BLDD015and BLDD026 respectively showing low uranium values in basalt, greywacke and andesite. It was also observed that the low uranium anomalies corresponded with low radiometric readings.

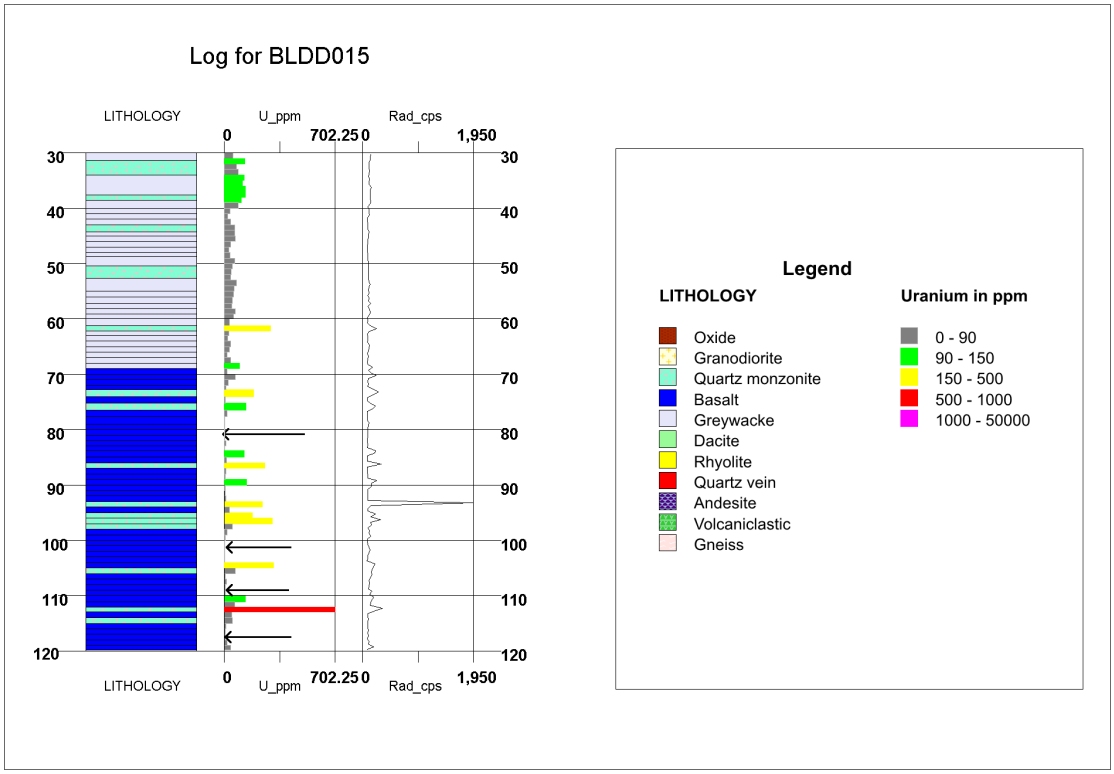

Figure 5.17 BLDD015 Showing Low U Values in Greywacke and Basalt

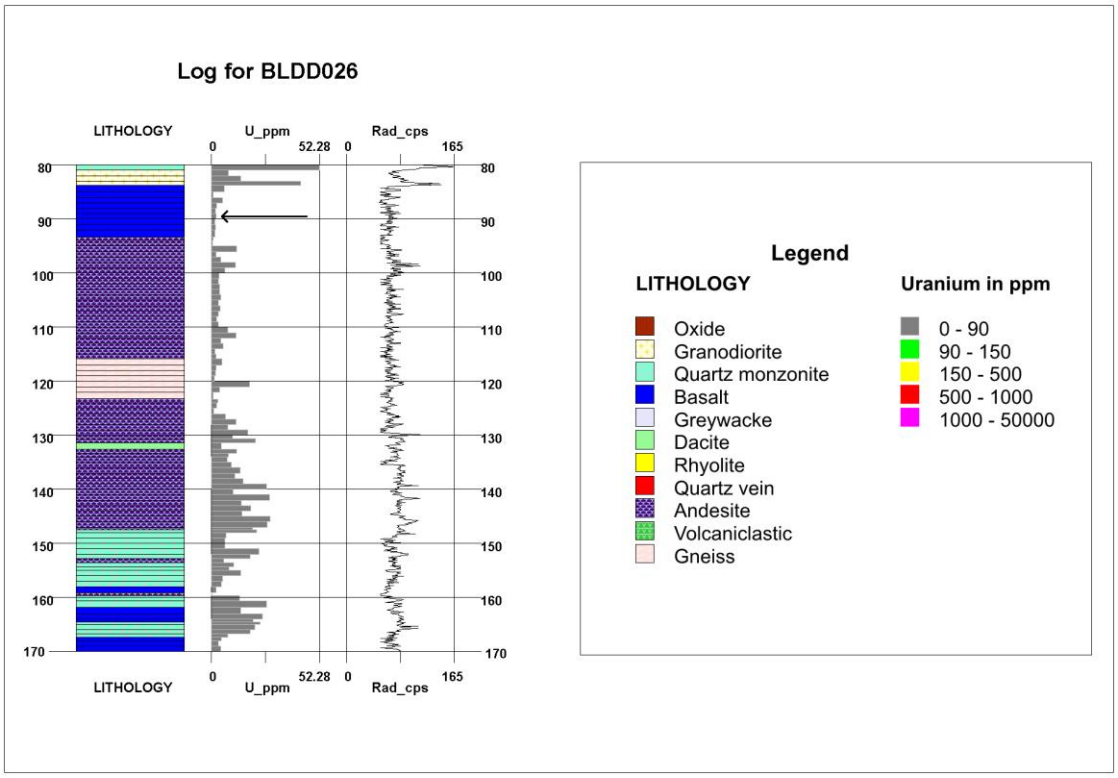

Figure 5.18 Basalt and Andesite Showing Low U Values in BLDD026

5.3.2 Uranium Anomalies

At Anomaly E, uranium mineralisation occur as torbenite (U-Cu phosphate) within the quartz monzonite and rhyolite units. High concentrations were detected in fractured zones and along lithological contact. These high concentrations also corresponded with strong radiometric anomalies. This is evident from the strip logs from BLDD024 and BLDD030 shown in Figure 5.19 and Figure 5.20 respectively.

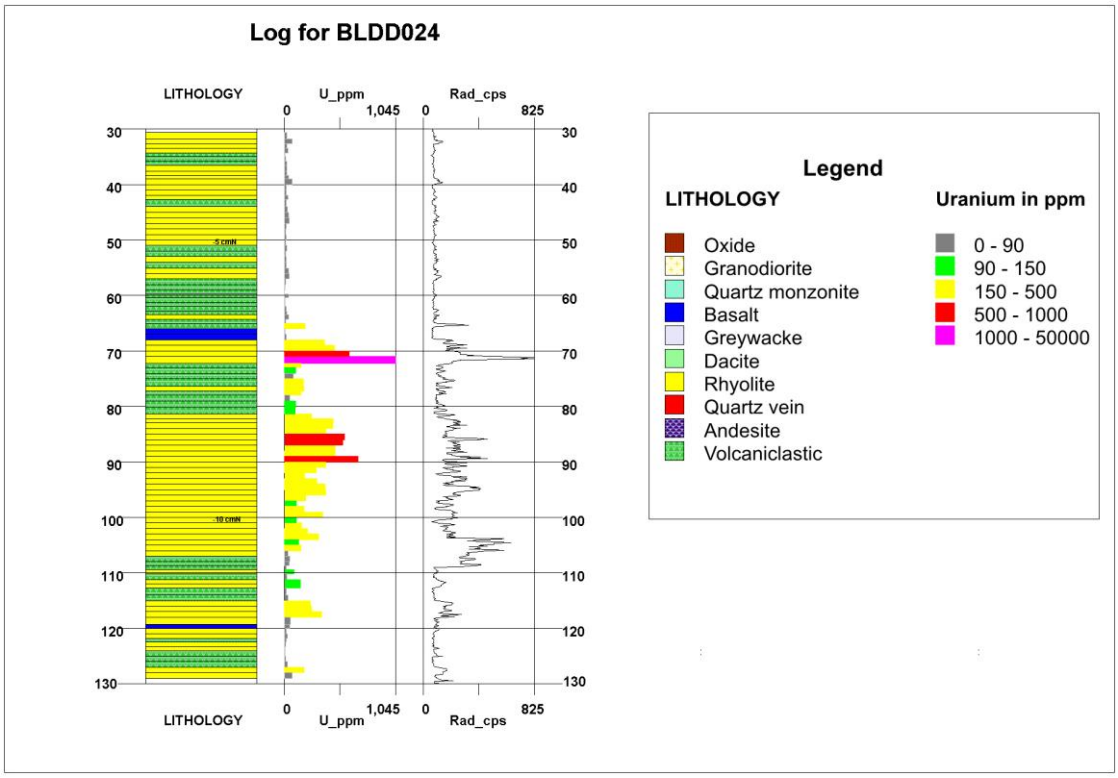

Figure 5.19 Rhyolite Showing High Uranium Anomalies in BLDD024

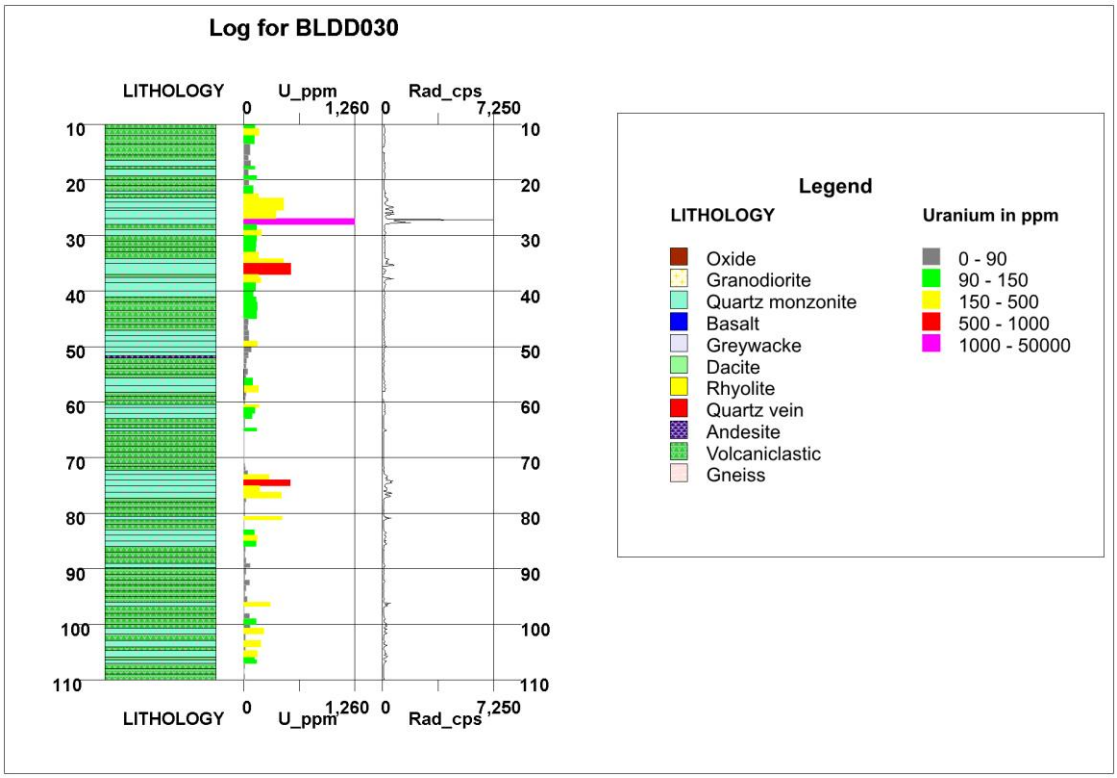

Figure 5.20 High Uranium Anomalies in Quartz Monzonite in BLDD030

Maximum value of 2043.7 ppm of uranium was recorded in the quartz monzonite. High anomalous values were also recorded within the rhyolite unit and along contact and fractured zones. This is due to the mobility of uranium in such units.

5.3.3 Uranium anomalies and radiometric readings

A strong direct correlation between uranium anomalies and the radiometric counts per second recorded by the SPP2 NF Scintillometer was observed in the strip logs for the diamond drill holes in area E. Not only does uranium anomalous intervals give high radiometric readings, the absolute value of the anomaly in part per million (ppm) is proportional to the strength of the radiometric count per second. Typical observations are given in Figure 5.21 and Figure 5.22 where BLDD033 and BLDD016

The correlation between the radiometric reading and the uranium anomalies indicates that the radiations picked up by the Scintillometer are from uranium sources, and not thorium or potassium sources

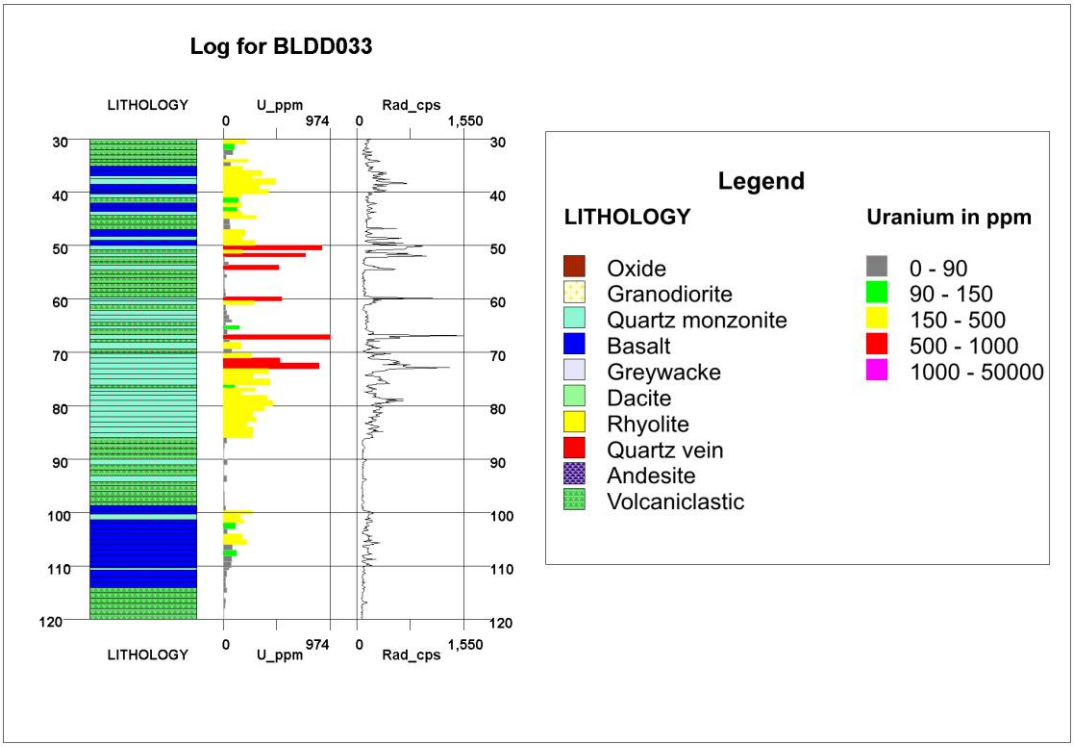

Figure 5.21 BLDD033 Showing Direct Correlation between Uranium Anomalies and Radiometric Cps

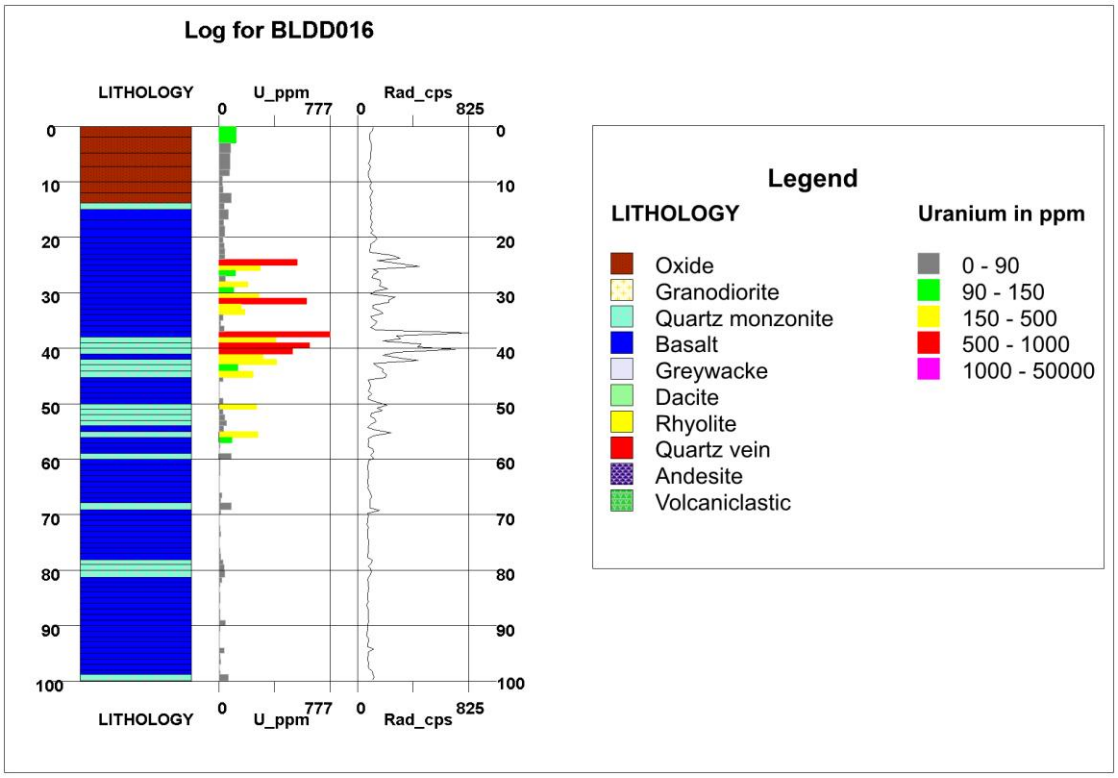

Figure 5.22 BLDD016 Showing Direct Correlation between Uranium Anomalies and Radiometric Cps

5.4 Delineation of Anomaly

Since a correlation was established between the radiometric readings and laboratory assay results for uranium, mineralised zones were delineated using both the radiometric counts per second and the laboratory assay results.

Five mineralisation corridors were delineated at area E, using radiometric readings (see Figure 5.23), and it these coincide exactly with mineralised corridors defined using laboratory assay results for uranium, as shown in Figure 5.24.

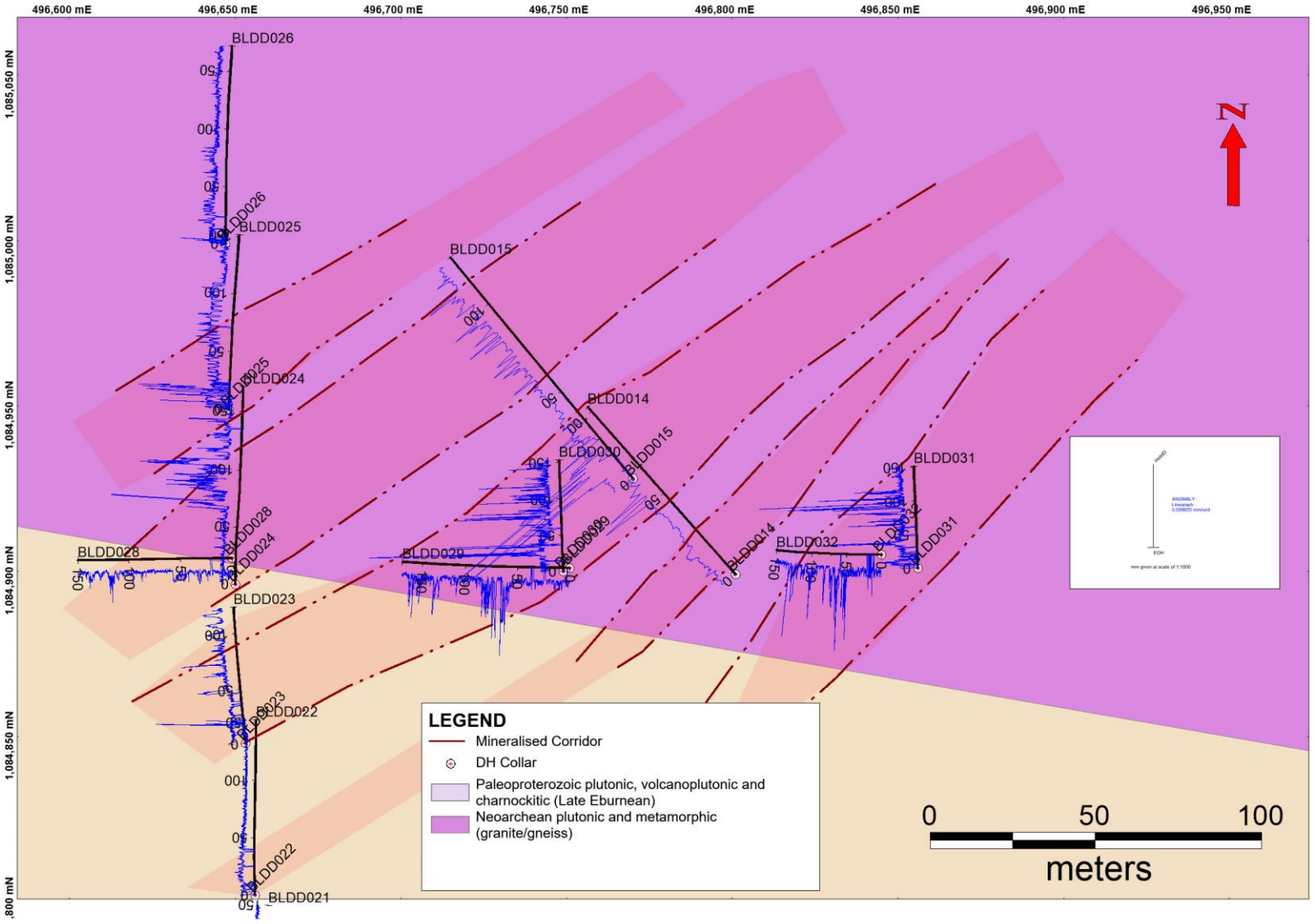

Figure 5.23 **Mineralisation Corridors defined by Radiometric Cps**

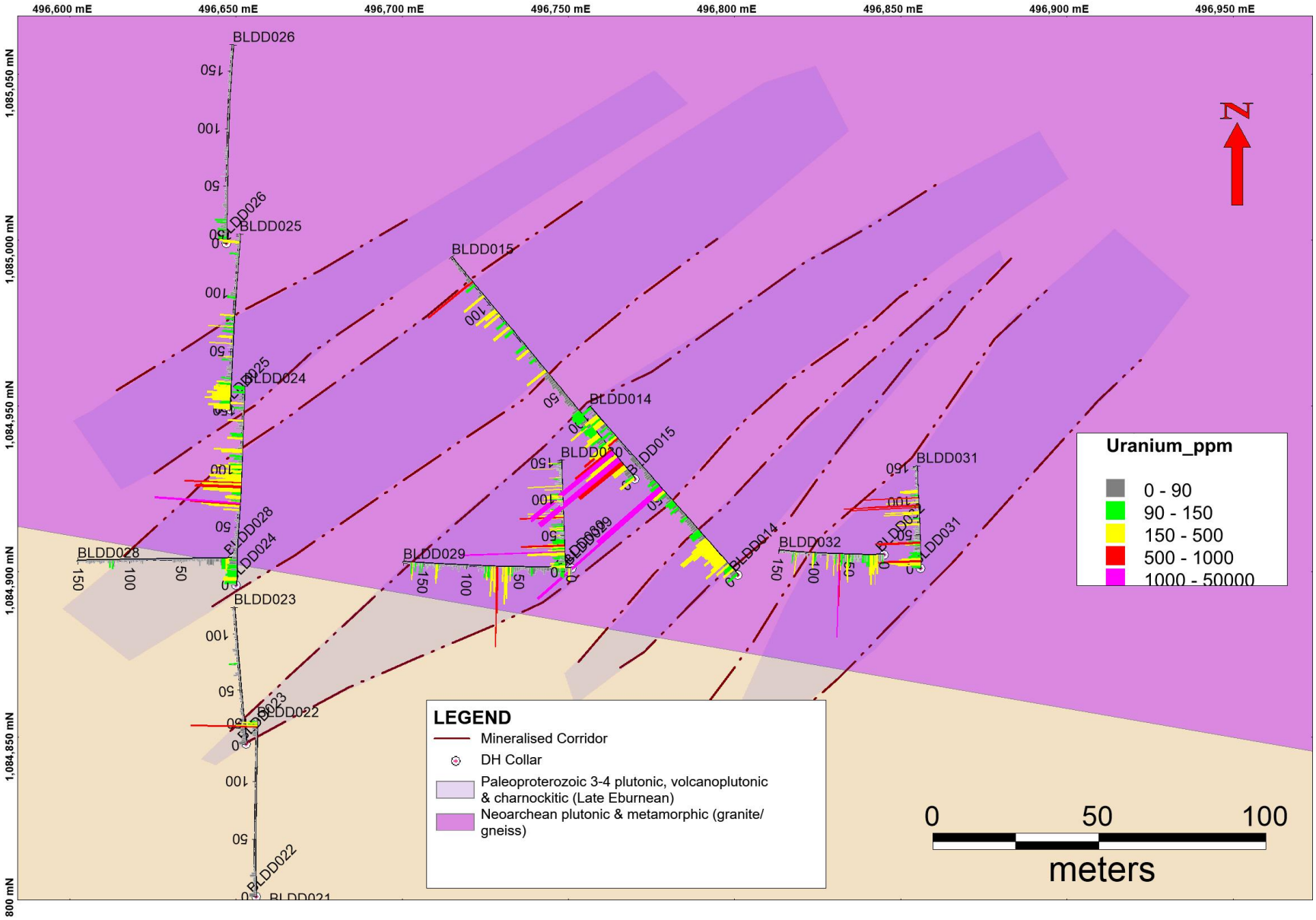

Figure 5.24 Mineralisation Corridors Defined by Laboratory Assays

CHAPTER 6

CONCLUSIONS AND RECOMMENDATIONS

6.1 Conclusions

At the CPP area, negative magnetic susceptibility recorded at near surface residual quartz zones returned anomalous gold values, but only three drillholes encountered such zones. Interval with low magnetic susceptibility returned both anomalous and non-anomalous gold values. High magnetic susceptibility intervals also showed varied assay results, elevated gold values were recorded in certain area whilst others yielded no anomalies.

No correlation could be established between gold mineralisation and magnetic susceptibility in the CPP area of Balatindi. Magnetic susceptibility therefore, cannot be used to delineate gold anomalies in Balatindi.

At anomalies A to E areas, a strong direct correlation was established between the radiometric count per second recorded with the SSP2 NF Scintillometer and uranium anomalies from assay results. Therefore, it is concluded that the radiometric count per second recorded is from a uranium source and thus the SPP2 NF Scintillometer can be used to delineate anomalous interval on drill core for exploration purpose.

Five mineralisation corridors delineated using the radiometric counts per second compared similarly with the mineralisation corridors delineated using uranium assay results from the laboratory

The rapid manner in which the SPP2 NF Scintillometer picks up anomalous intervals with certainty makes radiometric survey a faster and cheaper way of delineating uranium anomalies within the Area E part of the Balatindi property.

6.2 Recommendations

The fact that certain intervals with very high magnetic susceptibility returned anomalous gold grades could be an indication that gold mineralisation predates the magnetite banding in the area.

It is recommended that Heavy Mineral Concentration Analysis be carried out on the mineralised magnetite bands so to understand the relationship between the heavy magnetite and gold mineralisation.

It is further recommended that paragenesis analysis be carried out between gold mineralisation and magnetite banding in the CPP area to better understand the age relationship between the magnetite banding and gold mineralisation.

REFERENCES

Anon. (1979, "Gamma Ray Surveys in Uranium Exploration", *Technical Reports Series No. 186*, IAEA, Vienna, 90pp.

Anon. (1989), "Construction and Use of Calibration Facilities for Radiometric Field Equipment", *Technical Reports Series No. 309*, IAEA, Vienna, 123pp.

Anon. (1991), Recommendations of the International Commission on Radiological Protection, *ICRP Publication 60*, Pergamon Press, Oxford, 12p.

Anon. (1992a), "Atomic and Nuclear Physics", *ISO 31-9*.

Anon. (1992b), "Nuclear Reactions and Ionizing Radiation", *ISO 31-10*.

Anon. (1993), Protection against Radon-222 at Home and Work, International Commission on Radiological Protection, *ICRP Publication 65*, Pergamon Press, Oxford, 45pp.

Anon. (1999), "Social and labour issues in small scale mines. *TMSSM/1999*, International Labour Organisation 99 pp.

Anon. (2003). IAEA. *Guidelines for radioelement mapping using gamma ray spectrometry data*, IAEA., Vienna, 150pp.

Anon. (2009), "Abitibi Geophysics,"Detailed Ground Radiometric Survey, Rcu And Hpu Properties,Roberts-Creelman And Hyman-Porter Townships", *Unpublished Report, Abitibi Geophysics*, 10 pp.

Anon. (2010). Burey Gold Ltd, Unpublished *Balatindi First Quarter Report.*, 97pp.

Boroomand, A. M., Safari, A., and Bahroudi, A. (2015), "Magnetic susceptibility as a tool for mineral exploration (Case study: Southern of Zagros Mountains)", *Int. J. Min. and Geo-Eng.* Vol. 49, pp. 57-66

Billa, M., Feybesse, J.L., Bronner, G., Lerouge, C., Mile´si, J.P., Traore´, S., Diaby, and S. (1999) "Les formations a` quartzites rubane´s ferrugineux des Monts Nimba et du Simandou: des unite´s empile´es tectoniquement, sur un soubassement plutonique

Arche´en (craton de Ke´ne´ma–Man), lors de l'oroge`ne eburne´en. C.R. Acad" *Sci.Paris Sci*, Terre Planet 329, pp. 287–294.

Bonhomme, M. (1962), "Contribution a` l'e´tude ge´ochronologique de la plate-forme de l'Ouest africain", *The`se. Ann. Fac. Sci. Univ. Clermond-Ferrand*, Fr., Ge´ol. Mine´ral 5, p. 62.

Bleil, U., and N. Petersen (1982), Magnetic properties of natural minerals,in Numerical Data and Functional Relationships in Science and Tech-nology, Group V: Geophysics and Space Research, edited byG. Angenheister, pp. 308 – 365, Springer, New York

Camil, J., Tempier, P., and Pin, C. (1983), "Age libe´rien des quartzites a` magne´tite de la re´gion de Man (Coˆ te d'Ivoire) et leur place dans l'oroge`ne libe´rien. C.R.Acad", *Sci. Paris*, Vol. 296, pp. 149–151.

Cocherie, A., Legendre, O., Peucat, J.J. and Kouamelan, A. (1998), "Geochronology of polygenetic monazite constrained by in situ electron microprobe Th–U–total Pb determination: implications for Pb behaviour in monazite", *Geochim. Cosmochim.* Acta 62, 2475–2497.

Coker, J. O., Amidu .O. Mustapha, A. O., Makinde, V., and Adesodun, J. K. (2013), "Application of Radiometric Surveys to Delineate between Sedimentary Terrain and Basement Complex: A case study of Sagamu and Abeokuta, South Western Nigeria", *Journal of Natural Sciences Research*, Vol.3, pp. 13-16.

Clark, D.A. (1997), "Magnetic properties of rocks and minerals", *AGSO Journal of Australian Geology and Geophysics*, Vol. 17.

Egal, E., Thie´blemont, D., Lahonde`re, D., Guerrot, C., Costea, C. A., Iliescu, D. and Delor, C. (2002), "Late Eburnean Granitization and Tectonics along the Western and Northwestern Margin of the Archean Kenema–Man domain (Guinea, West African Craton)", *Precambrian Research*, pp 57–84.

Evans, M., and Heller, F. (2003), *Environmental magnetism. Principles* and *Applications of Enviromagnetics*, Elsevier Academic Press, 54 pp

Gabor, P., and Peter, V. (2011), *Geophysics 2,* Digitalis Egyetem, Terv, 16 pp

Gemail Kh., Abd-El Rahman, N. M. and Giath, B. M. (2016), "Integration of ASTER and Airborne Geophysical Data for Mineral Exploration and Environmental Mapping: A case study, Gabal Dara, North Eastern Desert, Egypt. *Environ Earth Sci*, 10 pp.

Goujou, J.C., Thie´blemont, D., Delor, C., Cocherie, A., Lacomme, A., Lafon, J.M., Tegyey, M., The´veniaut, H., Sall, H., Souare´, S., Toure´, J., Bah, M., Balde´, A. and Sane´, H. (1999), "BRGM, DNRGH, Notice explicative de la Carte ge´ologique de la Guine´e a` 1/200 000; Feuille no. 30, Macenta. Conakry (GIN)" *Ministe`re des Mines, de la Ge´ologie et de l'Environnement*, 22 p.

Grenholm, M. (2014), The Birimian Event in the Baoulé Mossi Domain (West African Craton) - regional and global context, *Dissertations in Geology at Lund University*, No. 375, 111 pp.

Heidelberg L.B. (1986), "Numerical Data and Functional Relationships in Science and Technology, *New Series, II/16*, Diamagnetic Susceptibility, Springer-Verlag, 255pp.

Hirdes, W., Davis, D.W. and Eisenlohr, B.N. (1992), "Reassessment of Proterozoic Granitoid Ages in Ghana on the Basis of U/Pb Zircon and Monazite Dating", *Precambrian Res.*, Vol. 56, pp. 89–96.

Hirdes, W., Davis, D.W., Lu¨ dtke, G. and Konan, G. (1996), "Two generations of Birimian (Paleoproterozoic) volcanic belts in northeastern Coˆ te d'Ivoire (West Africa): consequences for the ''Birimian controversy'', *Precambrian Res.*, Vol. 80, pp. 173–191.

Hrouda, F., and Kahan, Š. (1991), "The Magnetic Fabric Relationship between Sedimentary and Basement Nappes in the High Tatra Mountain", *N. Slovakia. J. Struct. Geol.*, pp 431-442.

Hrouda, F., Chlupacova, M., and Chadima, M. (2009), "The Use of Magnetic Susceptibility of Rocks in Geological Exploration", *GEORADIS*, pp 23-50.

Hurley, P.M., Leo, G.W., White, R.W. and Fairbairn, H.W. (1971), "Liberian Age Province (about 2700 My) and Adjacent Provinces in Liberia and Sierra Leone. *Geol. Soc. Am.Bull.*, Vol. 82, pp. 3483–3490.

Kesse, G. O. (1985), *The Mineral and Rock Resources of Ghana*, Balkema Publ., Rotterdam, 610 p.

Lindsley, H, Andreasen, D. E., and Balsley, J. (1966), "Section 25: Magnetic properties of rocks and minerals", *10.1130/MEM97*, 543 p.

Kouamelan, A.N., Delor, C.and Peucat, J. J. (1997), "Geochronological Evidence for reworking of Archean Terrains during the Early Proterozoic (2.1 Ga) in the Western Coˆ te d'Ivoire (Man Rise-West African Craton)", *Precambrian Res*. Vol. 86, 177–199.

Kuma, J., Al-Hassan, S., Stainforth, B., and Thompson, F. (1999), "Magnetic Susceptibility of Rock Units in the Bogosu Gold Limited Concession, Western Region, Ghana", *Ghana Mining Journal*, Vol. 5, pp 11-17.

Lafleur, J. (2006), "The North Shore Property Turgeon, Weegee, Highway pontbriand and Ne Costebela Le Claim Blocks, *NI 43-101 Technical Report*, Quebec: unpublished.

Lahonde`re, D., Lacomme, A., Le Berre, P., Iliescu, D., Guerrot, C., Cocherie, A., Diabate´, B., Gaye, F., Thie´blemont, D., Minthe´, D. and Feybesse, J. L. (1999), "BRGM, DNRGH. Notice explicative de la Carte ge´ologique de la Guine´e a` 1/200 000, Feuille no. 27–28, Damaro-Odienne´. Conakry (GIN), *Ministe`re des Mines, de la Ge´ologie et de l'Environnement*, 22 pp.

Lowe, K. (2012), Resource Estimate Update Mansounia Gold Deposit Guinea, West Africa, *Unpublished Report*, 59 pp.

Murakami, H. (2007), "Variations in Chemical Composition of Clay Minerals and Magnetic Susceptibility of Hydrothermally Altered Rocks in the Hishikari Epithermal Gold Deposit SW Kyushu, Japan"', *Resource Geology Vol. 58, No. 1*, pp. 1-24.

Palm, Eric (2011). "Tesla". National High Magnetic Field Laboratory", *http://www.magnet.fsu.edu/education/tutorials/magnetminute/tesla-transcript.html*, Date Assessed: October 2011.

Plimer, I. (1985), *Submarine exhalative ores*, Geol. Survey of Czechoslovakia, Prague.

Plunkett, M. J. (1991), "Tools and Techniques in Radiometric Exploration", *Geotech*, pp 1-4.

Ramadan, T. M, El Mongy, S. A., Salah El Dein, S. (2002), "Exploration for Uranium and Thorium Mineralisations at Wadi Um Laseifa Area, Central Eastern Desert, Egypt:Using Remote Sensing Technique",

Ransome, I., (2004). The Balatindi Gold Prospect, Republic of Guinea, a Discussion Comment. Unpublished Report,

Robertson, M., and Witleey, J. (2013), "Balatindi Project, Independent Review of the Mineral Resource Potential and Geological Model", *Unpublished Report*, The MSA Group,

Tarling, D., and Hrouda, F. (1993), *The Magnetic Anisotropy of Rocks*, Chapman and Hall, London, UK.

Thie´blemont, D., Delor, C., Cocherie, A., Lafon, J.M., Goujou, J.C., Balde´, A., Bah, M., Sane´, H., Fanning, M.A. (2001), "3.5 ga granite-gneiss basement in Guinea: further evidence

for early Archean accretion within the west african Craton, *Precambrian Res.*, Vol. 108, pp. 179–194.

Tsiboah, T., and Arko, J. (1999). Magnetic Susceptibility Index Measurement and Its Implication for Gold Exploration at Ashanti Mine, Obuasi, *Ghana Mining Journal*, *5*, 22-29.

Wemegah, D. M. (2009), "Magnetic Susceptibility Characterization of Mineralized and Non-Mineralized Rocks from the Subenso Concession of Newmont Ghana Gold", *Ghana Science Association Biennial Conference*, p. 45.

Wemegah, D. M., Menyeh, A., and Danour, S. K. (2009b), "*Magnetic Susceptibility Characterization of Mineralized and Non-Mineralized Rocks from the Subenso Concession of Newmont Ghana Gold, Ghana Science Association Biennial Conference*, University of Cape Coast, 4th – 9th August, 2009.

Wemegah, D. D., Preko1, K., Noye,R. M., Boadi, B., Menyeh, A., Danuor, S. K., and Amenyoh, T. (2015), "Geophysical Interpretation of Possible Gold Mineralization Zones in Kyerano, South-Western Ghana Using Aeromagnetic and Radiometric Datasets, *Journal of Geoscience and Environment Protection*, Vol. 3, pp. 67-82

INDEX

G

Q